MOUNTAIN-PLAINS CONSORTIUM

MPC 21-426 | J. Seo, B. Kidd, and N. Wehbe

Field and Analytical Study for Deteriorating Precast Double-Tee Girder Bridges

MOUNTAIN-PLAINS CONSORTIUM REGION 8

A University Transportation Center sponsored by the U.S. Department of Transportation serving the Mountain-Plains Region. Consortium members:

Colorado State University
North Dakota State University
South Dakota State University
University of Colorado Denver
University of Denver
University of Utah
Utah State University
University of Wyoming

Technical Report Documentation Page

1. Report No.	2. Government Accession No.	3. Recipient's Catalog No.
MPC-565		

4. Title and Subtitle	5. Report Date
Field and Analytical Study for Deteriorating Precast Double-Tee Girder Bridges	January 2021
	6. Performing Organization Code

7. Author(s)	8. Performing Organization Report No.
J. Seo B. Kidd N. Wehbe	MPC 21-426

9. Performing Organization Name and Address	10. Work Unit No. (TRAIS)
Department of Civil and Environmental Engineering South Dakota State University Brookings, South Dakota	11. Contract or Grant No.

12. Sponsoring Agency Name and Address	13. Type of Report and Period Covered
Mountain-Plains Consortium North Dakota State University PO Box 6050, Fargo, ND 58108	Final Report
	14. Sponsoring Agency Code

15. Supplementary Notes

Supported by a grant from the US DOT, University Transportation Centers Program

16. Abstract

The ultimate goal of this project is to provide a better understanding of structural performance of in-service DT bridges loaded with actual trucks. The objectives of this project to achieve this goal are: 1) To identify damage of typically used DT bridges; 2) To determine live-load distribution and dynamic load allowance factors of the DT bridges; and 3) To investigate load-carrying capacity of the DT bridges.

17. Key Word	18. Distribution Statement
highway bridges, live loads, structural analysis, truck traffic	Public distribution

19. Security Classif. (of this report)	20. Security Classif. (of this page)	21. No. of Pages	22. Price
Unclassified	Unclassified	76	n/a

Field and Analytical Study for Deteriorating Precast Double-Tee Girder Bridges

Junwon Seo, Ph.D, PE
Brian Kidd, B.S., EIT
Nadim Wehbe, Ph.D, PE

Department of Civil and Environmental Engineering
South Dakota State University
Brookings, South Dakota

January 2021

Acknowledgments

The authors would like to thank the Mountain-Plains Consortium (MPC) University Transportation Center for providing the funding for this research. The authors would also like to thank Mr. Sandip Rimal, Mr. Zach Gutzmer, and Dr. Mostafa Tazarv for their help with field testing. The authors would also like to acknowledge the South Dakota Department of Transportation for their help with the field tests and providing the truck and equipment used during the field tests.

Disclaimer

ABSTRACT

This project discusses the performance of deteriorating double-tee (DT) girder bridges that have been in service for many years. This included field testing of two single-span DT girder bridges in South Dakota for live load distribution factors (LLDFs) and dynamic load allowance (IM). The LLDFs and IM were determined using strain data measured during the tests. When calculating LLDFs, nearly all the measured LLDFs were below the American Association of State Highway Transportation Officials (AASHTO) values. While analyzing the data, it was found that the stems on the same girder did not always have similar strain quantities. Hence, newly proposed stem and joint approaches to calculate the LLDFs were investigated and compared with the conventional girder approach. These results were also compared with those determined according to AASHTO Standard and Load and Resistance Factor Design (LRFD) specifications. It was found that both the AASHTO LRFD and Standard specifications were conservative when estimating IM, compared with the test results for both bridges. Analytical models for both bridges were then created in CSi Bridge to perform parametric studies with variance in DT bridge design parameters. It was concluded that the AASHTO LRFD values are typically conservative for the studied parametric bridges.

TABLE OF CONTENTS

LIST OF TABLES

LIST OF FIGURES

EXECUTIVE SUMMARY

Two deteriorating double-tee (DT) girder bridges (including Bridge A with 762-mm deep DT girders and Bridge B with 584-mm deep DT girders) in South Dakota, both over 30 years old, were field tested with a static and dynamic load. From the recorded strain data, the field live-load distribution factors (LLDFs) and dynamic load allowance (IM) factors were calculated. The American Association of State Highway Transportation Officials (AASHTO) Load and Resistance Factor Design (LRFD) and AASHTO Standard specifications were compared with the field LLDFs and IMs. It was determined that the AASHTO LRFD specifications were conservative for the tested DT girder bridges, with two exceptions. An exterior DT girder on Bridge A and an interior DT girder on Bridge B exceeded the AASHTO LRFD LLDFs by 2.6% and 2.9%, respectively. The AASHTO Standard codified LLDFs were significantly higher than the field LLDFs in all cases. The AASHTO LRFD and AASHTO Standard specifications were conservative by at least 50% when calculating the IM factors in all instances for the two deteriorating DT bridges.

The strain data from the field tests were analyzed for LLDFs in three different approaches: girder approach, stem approach, and joint approach. The LLDFs calculated from each of the approaches were then compared with those determined based on the AASHTO LRFD and AASHTO Standard specifications. The girder approach had an average percent difference of 34% and 91% when compared with the AASHTO LRFD and AASHTO Standard specifications, respectively. The joint approach produced average percent differences similar to the girder approach, but the stem approach was the most conservative approach. In addition, finite element models were also created in CSi Bridge and calibrated with the measured strain data. The effects of design parameters, encompassing span length, deck width, concrete strength, use of diaphragms, and width-length ratio, were investigated on the LLDFs. The LLDFs decreased as the span length increased. The interior LLDF decreased by 10.8% per 6.1 m of span, on average, for Bridge A; the exterior LLDF decreased by an average of 8.1% per 6.1 m of span. The interior LLDF decreased by 8.5% per 6.1 m of span, on average, for Bridge B; the exterior LLDF decreased by 5.8% per 6.1 m of span, on average. The other parameters showed insignificant changes in the LLDFs. The AASHTO LRFD interior LLDFs were consistent with the analytical LLDFs. However, when Bridge B had a span length less than 12.2 meters, the AASHTO LRFD LLDFs were exceeded by the analytical LLDFs.

1. INTRODUCTION

1.1 Background and Problem Statement

Across the United States, there are many DT bridges in service on local road networks. Through inspection, it has been found that rapid deterioration of longitudinal joints between DT girders frequently occurs. This deterioration can significantly degrade the structural performance of these DT bridges. Some studies (Wehbe et al. 2016) attempted to perform laboratory tests of full-scale DT girder specimens to examine their ultimate and fatigue performance. Specifically, Wehbe et al. (2016) found that under fatigue loadings, the DT girder specimen with a conventional joint representing an actual DT bridge quickly deteriorated due to cracks along the longitudinal joint.

Laboratory tests have demonstrated the structural performance of the DT girders. However, there is a lack of studies focusing on integrated field testing with visual inspection and structural analysis for the evaluation of existing DT bridges. The results from the laboratory testing cannot directly be used to determine the actual structural performance of existing DT bridges due to the discrepancy in remaining structural capacity and loading condition between laboratory and field tests. Generally speaking, existing DT bridges quickly deteriorate over time with increasing traffic demands. It is necessary to examine the current, in-service performance of existing DT bridges subjected to rating trucks with known weights and configurations.

1.2 Objectives

The goal of this project was to better understand the structural performance of two representative in-service DT bridges with significant deterioration. The damage typically found on the two DT bridges was examined and quantified, and their LLDFs and IMs were then determined through field tests with a known truck. The LLDFs of DT bridges with varying parameters will also be investigated by using calibrated analytical models.

1.3 Project Scope and Organization

To achieve the objectives previously mentioned, the following tasks were undertaken in this work:

1) Conduct a literature review of the state or the art and practice in LLDFs and IMs, specifically on deteriorating DT girder bridges and/or other bridge types.
2) Inspect the two bridges selected for field testing to identify and quantify the damage status.
3) Conduct field testings on the two DT girder bridges.
4) Calculate the LLDFs and IMs of the two bridges and compare them to the AASHTO LRFD and AASHTO Standard specifications.
5) Create and calibrate finite-element models for the two DT bridges tested.
6) Conduct a parametric study regarding the impact that different variables have on the LLDFs.
7) Summarize the findings and conclusions.

This report is divided into eight sections. Section 2 is dedicated to the review of current literature on LLDFs and IMs on deteriorating DT bridges and/or other bridge types. Section 3 discusses the two bridges selected for the field testing and quantifies the damage present on both bridges. Section 4 provides the information on the field testing, including the truck configuration, truck paths, and instrumentation. Section 5 shows the strain data from the field tests and investigates the LLDFs and IMs of the two DT bridges. Section 6 compares the LLDFs and IMs from the field tests with the AASHTO LRFD and Standard specifications. Section 7 discusses the creation and calibration of the finite element models and the parametric study that was conducted on the two models. Section 8 consists of the summary of the research, along with the results, conclusions, and future work on this subject.

2. COMPREHENSIVE LITERATURE REVIEW

The literature review is presented in two sections: Section 2.1 discusses LLDFs and Section 2.2 discusses IM factors. Section 2.1 is separated into subsections based on the codified equations, effect of bridge parameters, effect of vehicle parameters, and LLDFs of DT bridges. Section 2.2 is divided in a similar manner.

2.1 LLDFs

2.1.1 Codified Equations

The estimation of LLDFs is not a new topic for the other bridge types (Zokaie 2000). The AASHTO Standard Specifications for Highway Bridges (AASHTO 1996) have included equations (entitled as "S-over" equations) for LLDFs since 1931. The past study led by Zokaie (2000) concluded that these equations were accurate only for common bridges (e.g., bridges with approximately 1.8 m girder spacing and a span length of 18 m) and deviated for short- and long-span bridges. In 1994, the AASHTO LRFD Bridge Design Specifications (AASHTO 2012) modified equations for the determination of LLDFs for interior and exterior girders. Compared with the AASHTO Standard, the AASHTO LRFD equations included more bridge types and more variables to determine LLDFs. Some of these variables include spacing, span length, and longitudinal stiffness. However, it was reported that the AASHTO Standard and LRFD equations were developed based on studies that did not specifically include DT bridges (PCINE 2012).

2.1.2 Effect of Bridge Parameters

Many studies (Yousif and Hindi 2007; Hodson et al. 2012; Seo and Hu 2014; Seo et al. 2014a,b; Seo and Hu 2015; Seo et al. 2017) have attempted to estimate LLDFs of different types of bridges and compare them against the AASHTO code-compliant LLDFs. For instance, Yousif and Hindi (2007) compared the AASHTO LRFD LLDFs with a finite element model (FEM) of prestressed concrete I-girder bridges. The study reported the AASHTO LRFD LLDFs were sometimes over and under conservative with different girder spacing, span length, and slab thickness. Hodson et al. (2012) found that the AASHTO LRFD LLDFs were conservative for interior box girders but slightly non-conservative for exterior box girders. Kim and Nowak (1997) concluded that measured LLDFs are consistently lower than those of the AASHTO methods.

2.1.3 Effect of Vehicle Parameters

LLDFs may be a complex topic because the bridge configuration affects them; other parameters, such as the vehicle parameters, do as well. The LLDFs calculated by the AASHTO LRFD may not be representative of bridges with atypical vehicles traveling over them. Researchers (Seo and Hu 2014; Seo et al. 2014a,b; Seo and Hu 2015; Seo et al. 2017) have found that uncommon vehicle configurations, such as husbandry vehicles, can cause LLDFs that are higher than the AASHTO LRFD values.

2.1.4 LLDFs of DT Bridges

DT bridges have been commonly used on South Dakota local roads due to their ease of construction and cost-effectiveness. DT girders are placed side-by-side on the abutments, a welded steel plate connection is used to discretely connect the girders (usually spaced every 1.5 m), and the girder-to-girder keyway is filled onsite with a non-shrink grout. Previous studies (Wehbe et al. 2016; Tazarv et al. 2019) have demonstrated that this joint detailing is not sufficient for service and strength limit states and proposed

new detailing or rehabilitation techniques to improve the DT girder longitudinal joint performance. Damage of DT girder longitudinal joints is especially important in this study since this damage type affects the live load distribution between the girders. No previous field study has investigated LLDFs and IM for DT girder bridges with significant damage to the longitudinal joints.

There have been very few recent studies on the LLDFs of any DT bridges. Torres (2016) found that the AASHTO LRFD flexural LLDFs provided an accurate estimation for a DT bridge with significantly deteriorated flanges, implying it may be conservative for DT bridges without damage. Singh (2012) found that flexural LLDFs decrease as the DT span length increases, which agrees with the AASHTO LRFD equations for LLDFs. Huang and Davis (2018) used the current PCI guidelines for flexural LLDFs, which treat every stem as an independent girder, use the LLDF equation for a concrete I-girder bridge from the AASHTO LRFD, and use the average spacing between all the stems. This value is then doubled to consider a full DT girder, but this produces an over-conservative LLDF.

2.2 IM

2.2.1 Codified Equations

Dynamic Load Allowance (IM) factors consider the dynamic effect of a moving vehicle. When a vehicle drives over the bridge, the suspension system of the vehicle creates a vibration effect, causing the dynamic load from the vehicle to be greater than the static load of the vehicle. The AASHTO Standard (1996) and the PCI Bride Design Manual (PCI, 2003) included an equation for IM factors based on span length but set a maximum of 30%. The AASHTO LRFD (2012) specifies a constant value of 33% for the IM factor for ordinary bridges.

2.2.2 Effect of Bridge Parameters

IM is a factor of the span length, bridge stiffness, road surface condition, vehicle speed, and the vehicle suspension system. Deng et al. (2014) conducted a state-of-the-art review and found that the IM increases as the span length decreases and increases as the road surface condition worsens. Kim and Nowak (1997) concluded that IM factors decrease as the static strain increases, and that measured IM factors for large static strains are well below those of the AASHTO specifications.

2.2.3 Effect of Vehicle Parameters

IM factors may be even more complex than LLDFs. There are still some discrepancies, specifically, whether the characteristics of the truck affects the IM. The truck type can change IM significantly. Deng et al. (2014) concluded that the IM is independent of the number of axles on a vehicle. A previous study (Ashebo et al. 2007) also reported that IM decreases as the weight of the vehicle increases.

2.3 Analytical Study

There are many computer programs available to engineers for modeling bridges. There are very few analytical studies of DT girder bridges in the current literature. FEMs have been created for DT bridges using shell and link elements (Singh 2012; Torres 2016). Torres (2016) was also able to correctly model a DT bridge with deteriorated flanges by using link elements. Torres (2016) adjusted the shear stiffness of the link elements to represent the deteriorated flanges of the DT girders. Singh (2012) found that flexural LLDFs decrease as the DT girder span length increases, which agrees with the AASHTO LRFD equations for LLDFs.

Yousif and Hindi (2007) were successful in using SAP2000 to compare the AASHTO LRFD LLDFs with an FEM of prestressed concrete I-girder bridges. Huang and Davis (2018) created an FEM in ABAQUS and a simplified model in CSi Bridge and found good agreement between the two models. These studies suggest that CSi Bridge can be used to efficiently model DT girder bridges for this analytical work.

3. TEST BRIDGES

3.1 Bridge A

The first field testing was carried out on a single-span DT bridge, consisting of seven 762-mm-deep prestressed DT girders, on a gravel road. This DT girder is one of the standard sections used for DT bridges in South Dakota. The bridge span length was 11.6 meters. The bridge, which was located in Lincoln County, South Dakota, was 34 years old at the time of testing. Each of the girders, supported by concrete abutments, was 1.2-m wide and had a zero-degree skew angle. The girders were longitudinally connected using a steel plate connection and grouted shear key. Figures 3.1a and 3.1b show the road surface and bridge underneath, respectively.

(a) (b)

Figure 3.1 Description of Bridge A (Kidd et al. 2021): (a) view of the bridge from the road surface and (b) view from underneath the bridge

Figure 3.2 shows the damage map of the 762-mm-deep DT bridge observed before the field testing. The main bridge damage was the deterioration of the girder-to-girder joints, including leakage between joints, efflorescence, and corrosion of steel plates. Figure 3.3 shows an example of efflorescence on the 762-mm-deep girder bridge. Small spalling was also observed for some of the girder stems.

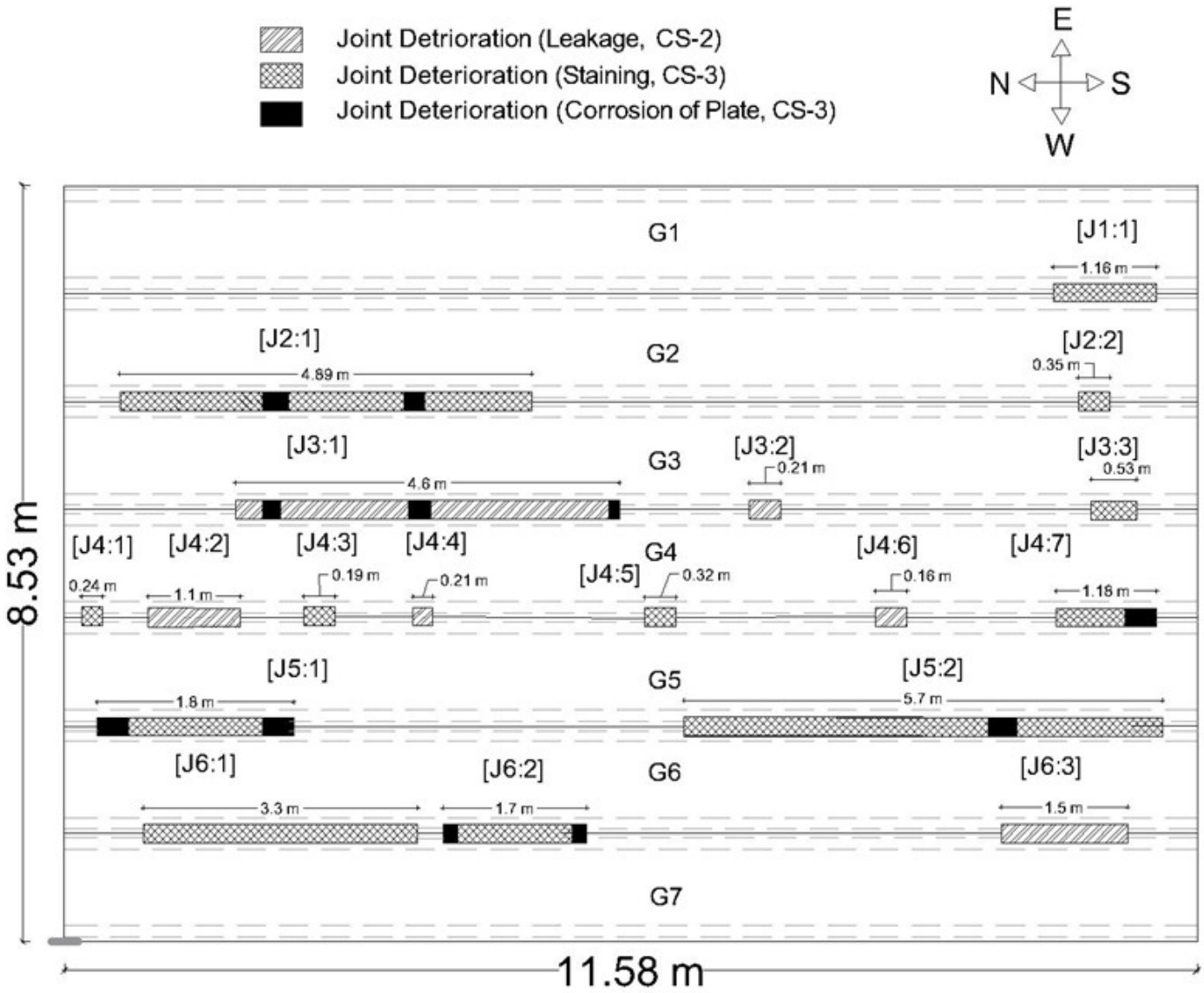

Figure 3.2 Damage of Bridge A from visual inspection

Figure 3.3 Efflorescence and erosion between G7 and G6 on Bridge A (Credit: Brian Kidd)

3.2 Bridge B

The second field testing was performed on another single-span, prestressed DT bridge but incorporating eight 584-mm-deep girders. The bridge span length was 15.24 m, and the bridge was simply supported on timber abutments with no skew angle. At the time of testing, this bridge had been in service for 38 years in Moody County, South Dakota. This is one of the standard DT girder sections used in South Dakota DT girder bridges. The bridge has a gravel wearing surface. Each girder was 1.17-m wide connected to the adjacent girder using a steel-plate connection and grouted joint. Figure 3.4 shows the road surface and a view from the bridge underneath.

Figure 3.4 Description of Bridge B (Kidd et al. 2021): (a) view of the bridge from the road surface and (b) view from underneath the bridge.

A visual inspection was conducted before the field tests, and Figure 3.5 shows the observed damage including the efflorescence and water leakage in the girder-to-girder joints. An example of the leakage is shown in Figure 3.6.

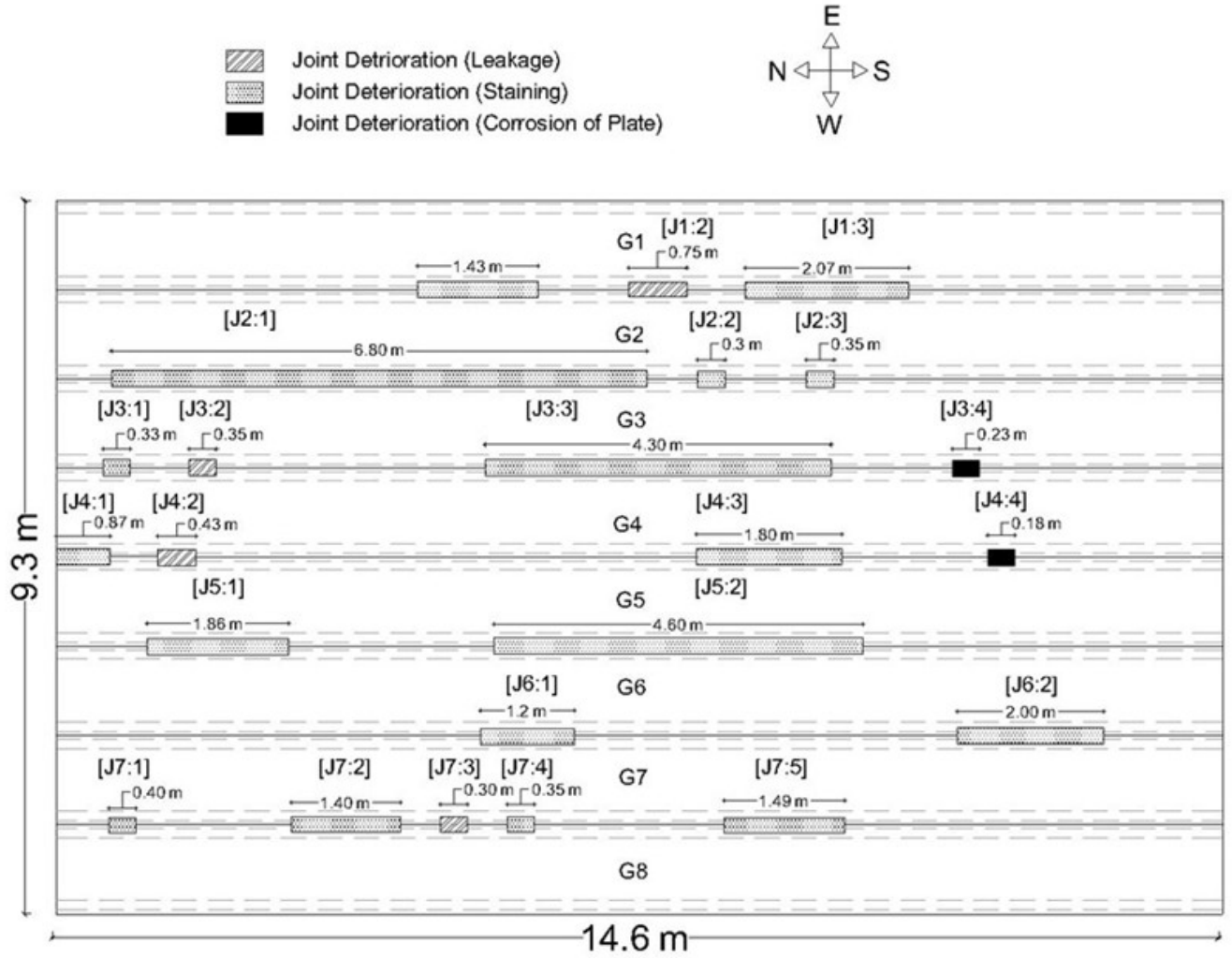

Figure 3.5 Damage on Bridge B from visual inspection

Figure 3.6 Example of efflorescence on Bridge B (Credit: Brian Kidd)

4. DAMAGE QUANTIFICATION

Damage quantification of bridge elements has yet to be standardized. Current practices use qualitative terms, encompassing severe, poor, fair, and good (AASHTO 2013). This method is subjective since it depends on the bridge inspectors and their judgment. To quantify the bridge damage, a new method was used to assign a numerical value to the qualitative terms. A visual inspection was necessary to measure the amount and type of damage. To quantify the damage, the damage was then given a weighted value based on the severity and amount of the damage. The entire process will be discussed in the following subsections.

4.1 Bridge Inspection

Before quantifying the damage, a visual inspection was performed on the bridges. The visual inspection was completed using tape measures, rulers, and a camera. Both the length and the thickness of the visible damage were measured. The visual inspection revealed damage at the longitudinal joints between the girders, but no significant damage on the girders themselves. Figures 4.1 and 4.2 show examples of longitudinal joint damage. Figure 4.1 shows an example of leakage through the joint, allowing water to seep through. Figure 4.2 shows an example of staining and corrosion in a joint. As stated before, Figures 3.2 and 3.5 show the location and type of the damage on Bridges A and B, respectively. It should be noted that the damage on Bridge A was measured using areas since the bridge clearance and water height allowed the research team to get close enough to the joints underneath the bridge. However, Bridge B had a deeper water level and a larger clearance; therefore, only the length was able to be measured. Note, the damage was identified and the affected area was measured by tape measure and ruler. The damage was identified based upon condition states (CS) stipulated by the AASHTO Manual for Bridge Element Inspection (AASHTO 2013).

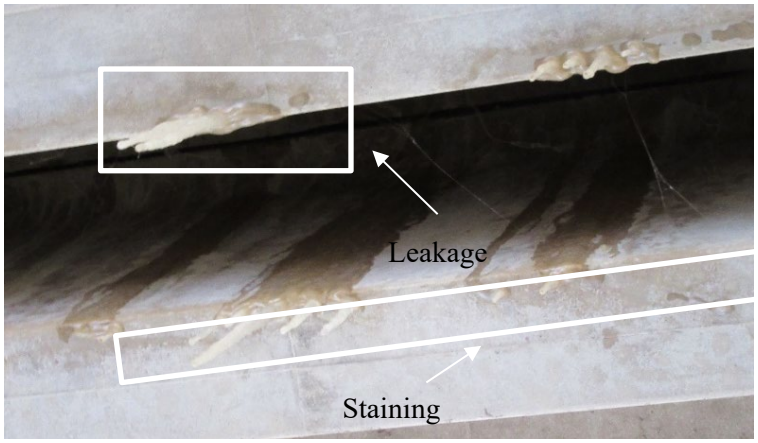

Figure 4.7 Example leakage in the joint allowing water in between girders (Credit: Brian Kidd)

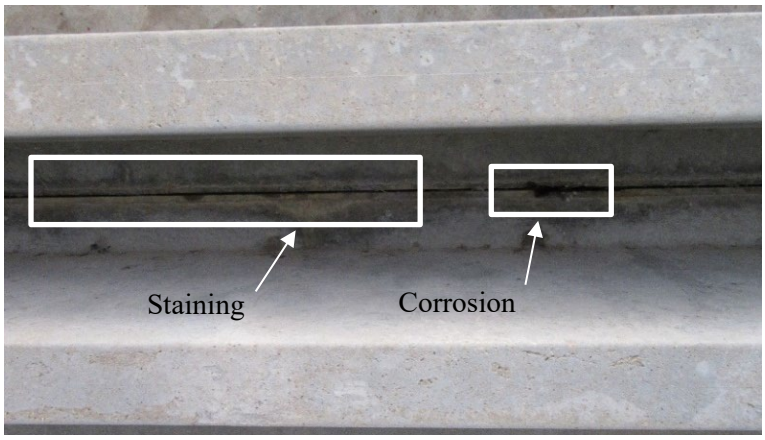

Figure 4.8 Sample staining and corrosion of the longitudinal joint (Credit: Brian Kidd)

4.2 AASHTO Manual Damage State

According to the AASHTO Manual for Bridge Element Inspection (AASHTO 2013), the elements of the bridges were inspected and classified as one of four CSs. Generally speaking, CS-1 means no damage, CS-2 is described as fair, CS-3 is a poor element state, and CS-4 is classified as severe damage. Once the visual inspection was completed and the AASHTO CSs were applied to the elements, the next step was to quantify the damage in terms of damage value adopted from the past study (Shinozuka et al. 2000). Using the damage value introduced by Shinozuka et al. (2000), a damage state was applied to each damage type. CS-1, CS-2, CS-3, and CS-4 were given damage values of 0, 0.3, 0.75, and 1, respectively. Table 4.1 shows the CS and corresponding damage values.

Table 4.1 Damage states used for damage quantification adopted from the past work (Shinozuka et al. 2000)

Condition State	Damage State	Damage Value
CS-1	None	0
CS-2	Fair	0.3
CS-3	Poor	0.75
CS-4	Severe	1

4.3 Damage Type, Portion, and Ratio

Detailed damage type, portion, and ratio from Bridge A and B are summarized in Tables 4.2 and 4.3, respectively, which can be seen on the damage maps shown in Figures 3.2 and 3.5. The first and second columns of Table 4.2 and 4.3 describe the damage location and type. Damage along the longitudinal joints included leakage, staining, and corrosion of the steel plates. When the grout in the joint deteriorates, water can get in the joint and leak through it. As it deteriorates more, efflorescence or staining occurs on the concrete below the joint. The joint includes a steel plate every 1.5 meters along the girder for both bridges. As the water penetrates the joint, it can accelerate the corrosion of the steel plates. For example, damage [J3:1] of Bridge A has both staining (S) and corrosion (C) present. The third columns of Table 4.2 and 4.3 show the amount of damage in terms of area. The portion was measured by hand using a tape measure. As mentioned previously, Bridge B only used the length of the damage because the large clearance and water level underneath the bridge did not allow the research team to get close enough to measure the width of the damage. Instance [J3:1] of Bridge A had 2932.3 cm^2 of staining and 153.2 cm^2 of corrosion at the joint. The AASHTO Manual (AASHTO 2013) for each damage instance is shown in

the fourth column of these tables. For example, damage [J3:1] of Bridge A was classified as poor (CS-3) for both staining and corrosion and given a damage state of 0.75 according to the past study (Shinozuka et al. 2000).

The damage portion (cm^2 or cm), determined by measuring the visual damage, was multiplied by the damage value introduced in (Shinozuka et al. 2000) to quantify the severity of the damage. This can be seen in column six of Tables 4.2 and 4.3. From the weighted damage area (the damage area multiplied by the damage value), a damage ratio was calculated by dividing the damage at each instance by the sum of the weighted damage areas for the entire bridge. For example, damage [J3:1] of Bridge A multiplied the damage amount by 0.75 for a weighted damage portion of 2314.1 cm^2. Then, 2314.1 cm^2 was divided by the total weighted damage portion (14196.9 cm^2) for a damage ratio of 0.163.

The damage ratios along the same longitudinal joint were summed to calculate the joint damage ratio (JDR) in column eight. To compare the damage ratio to the damage on the longitudinal joints, the JDR was converted to a girder damage ratio (GDR). The GDR represents the amount of longitudinal joint damage affecting the DT girder. The GDR was calculated by dividing the JDR by two and distributed equally to the adjacent DT girders. For example, the JDR on joint J3 of Bridge A was split between girders G3 and G4. The GDRs for both bridges, calculated from the values in Table 4.2 and 4.3, are shown in Table 4.4. It is worthwhile to note that this information was used in the calibration of the analytical studies, such that the link elements were given reduced shear stiffness values to match the AASHTO CS present on the longitudinal joints.

Table 4.2 Damage type, portion, and quantification from Bridge A

Location	Damage Type			Damage Portion (cm^2)			AASHTO Manual (AASHTO 2013)	Damage Value (Shinozuka et al. 2000)	Weighted Damage Portion (cm^2)	Damage Ratio	Joint Damage Ratio
	L	S	C	L	S	C					
[J1:1]	X	O	X	-	593.5	-	Poor	0.75	445.2	0.031	0.031
[J2:1]	X	O	O	-	2685.5	166.1	Poor	0.75	2138.7	0.151	0.159
[J2:2]	X	O	O	-	103.2	62.9	Poor	0.75	124.6	0.009	
[J3:1]	X	O	O	-	2932.3	153.2	Poor	0.75	2314.1	0.163	0.186
[J3:2]	O	X	X	129	-	-	Fair	0.3	38.7	0.003	
[J3:3]	X	O	X	-	387.1	-	Poor	0.75	290.3	0.020	
[J4:1]	X	O	X	-	116.1	-	Poor	0.75	87.1	0.006	0.093
[J4:2]	O	X	X	645.16	-	-	Fair	0.3	193.5	0.014	
[J4:3]	X	O	X	-	467.7	-	Poor	0.75	350.8	0.025	
[J4:4]	O	X	X	67.7	-	-	Fair	0.3	20.3	0.001	
[J4:5]	X	O	X	-	154.8	-	Poor	0.75	116.1	0.008	
[J4:6]	O	X	X	77.4	-	-	Fair	0.3	23.2	0.002	
[J4:7]	X	O	O	-	580.6	121	Poor	0.75	526.2	0.037	
[J5:1]	X	O	O	-	1625.8	61.3	Poor	0.75	1265.4	0.089	0.304
[J5:2]	X	O	O	-	3987.1	90.3	Poor	0.75	3058.1	0.215	
[J6:1]	X	O	X	-	2754.8	-	Poor	0.75	2066.1	0.146	0.226
[J6:2]	X	O	O	-	822.6	112.9	Poor	0.75	701.6	0.049	
[J6:3]	O	X	X	1445.2	-	-	Fair	0.3	433.5	0.031	

*Damage that is present is marked with an “O” and damage not present is marked with an “X”. “L” is leakage, “S” is staining, and “C” is corrosion.

Table 4.3 Damage type, portion, and quantification from Bridge B

Location	Damage Type			Damage Portion (cm)			AASHTO Manual (AASHTO 2013)	Damage Value (Shinozuka et al. 2001)	Weighted Damage Portion (cm)	Damage Ratio	Joint Damage Ratio
	L	S	C	L	S	C					
[J1:1]	X	O	X	-	143.3	-	Poor	0.75	107.5	0.044	
[J1:2]	O	X	X	75	-	-	Fair	0.3	22.5	0.009	0.117
[J1:3]	X	O	X	-	207.3	-	Poor	0.75	155.5	0.064	
[J2:1]	X	O	X	-	679.7	-	Poor	0.75	509.8	0.209	
[J2:2]	X	O	X	-	30	-	Poor	0.75	22.5	0.009	0.229
[J2:3]	X	O	X	-	35	-	Poor	0.75	26.3	0.011	
[J3:1]	X	O	X	-	33.3	-	Poor	0.3	9.99	0.004	
[J3:2]	O	X	X	35	-	-	Fair	0.3	10.5	0.004	0.148
[J3:3]	X	O	X	-	429.8	-	Poor	0.75	322.4	0.132	
[J3:4]	X	X	O	-	-	22.9	Poor	0.75	17.2	0.007	
[J4:1]	X	O	X	-	86.72	-	Poor	0.75	65.0	0.027	
[J4:2]	O	X	X	42.9	-	-	Fair	0.3	12.9	0.005	0.093
[J4:3]	X	O	X	-	179.8	-	Poor	0.75	134.9	0.055	
[J4:4]	X	X	O	-	-	17.8	Poor	0.75	13.4	0.005	
[J5:1]	X	O	X	-	186.2	-	Poor	0.75	139.7	0.057	0.199
[J5:2]	X	O	X	-	460.2	-	Poor	0.75	345.2	0.142	
[J6:1]	X	O	X	-	120.1	-	Poor	0.75	90.1	0.037	0.098
[J6:2]	X	O	X	-	199.5	-	Poor	0.75	149.6	0.061	
[J7:1]	X	O	X	-	40	-	Poor	0.75	30.0	0.012	
[J7:2]	X	O	X	-	140.2	-	Poor	0.75	105.2	0.043	
[J7:3]	O	X	X	30	-	-	Fair	0.3	9.0	0.004	0.116
[J7:4]	X	O	X	-	35	-	Poor	0.75	26.3	0.011	
[J7:5]	X	O	X	-	149.4	-	Poor	0.75	112.1	0.046	

*Damage that is present is marked with an “O” and damage not present is marked with an “X”. “L” is leakage, “S” is staining, and “C” is corrosion.

Table 4.4 Girder damage ratios

Girder	Bridge A	Bridge B
G1	0.016	0.059
G2	0.095	0.173
G3	0.173	0.188
G4	0.140	0.120
G5	0.199	0.146
G6	0.265	0.149
G7	0.113	0.107
G8	-	0.058

5. FIELD TESTS

5.1 Procedure

The research team conducted field tests on Bridges A and B described above. Both static and dynamic load tests using the South Dakota legal type 3 truck were performed on each bridge. The goal of the static load tests was to examine the flexural LLDFs of the bridges at the midspan, while the dynamic testing was intended to compare the dynamic response with the static response to calculate IMs. It should be noted that all the field testing data have been gained from the past literature (Kidd 2019; Kidd et al. 2021; Rimal et al. 2019, 2020).

Figure 5.1a and 5.1b show the truck paths for Bridges A and B, correspondingly. As part of the static load tests, the truck followed the paths at a crawl speed of 8 km/h. Note that the exterior paths (A and E) were offset by 0.61 meters from the edge of the exterior girder. The paths were chosen such that the truck axles would directly load two DT girders at a time, and all DT girders would be loaded at least once throughout the field testing. The identification of the DT girders, stems, and joints are also shown on these figures, as they will be used during the discussion of the LLDFs.

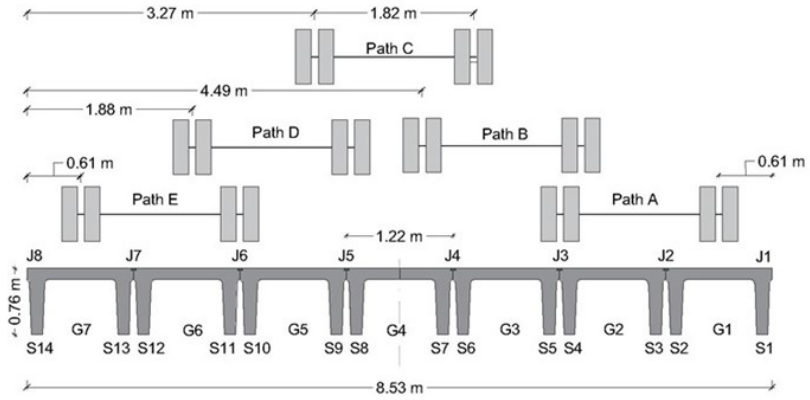

(a)

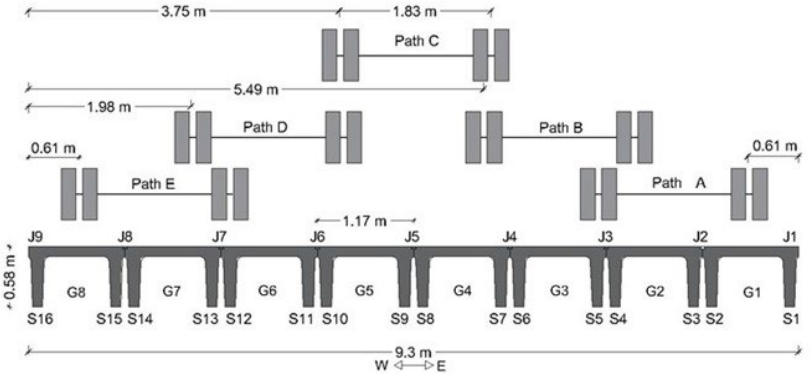

(b)

Figure 5.9 Truck passes for field testing: (a) Bridge A and (b) Bridge B

As stated above, the truck drove each pass at 8 km/h as a crawl speed loading. The truck was driven across the bridge at five different locations to see how the DT girders distribute loads on the bridge as shown in Figure 5.1a and 5.1b. The dynamic tests were tested at 56 km/h over the middle three paths (paths B, C, and D) because the gravel road did not allow the truck to correctly pass over Paths A and E at high speeds. Normally, a dynamic test uses a vehicle speed of 89 km/h; however, the gravel road made driving at 89 km/h in a large truck unsafe.

5.2 Instrumentation

Figures 5.2a and 5.2b show the field test instrumentation plan corresponding to Bridges A and B. The DT girder strains were collected using surface-mounted strain gauges. For Bridge A, one strain gauge was installed on each stem of all the DT girders at the bridge midspan for a total of 14 gauges. The strain was measured over a 305-mm length as recommended by the strain gauge manufacturer for concrete bridges. The same instrumentation plan was used for Bridge B. Due to the stem damage, strain gauges could not be placed at the bottom faces of a few stems. In those cases, the strain sensors were placed on the side of the girder, as close as possible to the bottom. Figure 5.3 shows an example of two strain gauges installed on DT girders at the midspan. This placement was chosen to get the largest strain values possible during the field test.

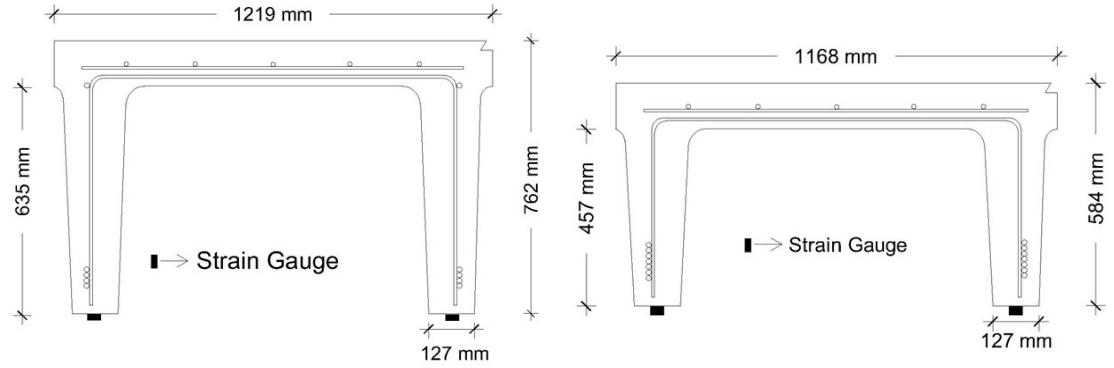

(a) (b)

Figure 5.10 Location of strain gauges on both bridges tested (Kidd et al. 2021): (a) Bridge A with 762-mm-deep DT girders and (b) Bridge B with 584-mm-deep DT girders

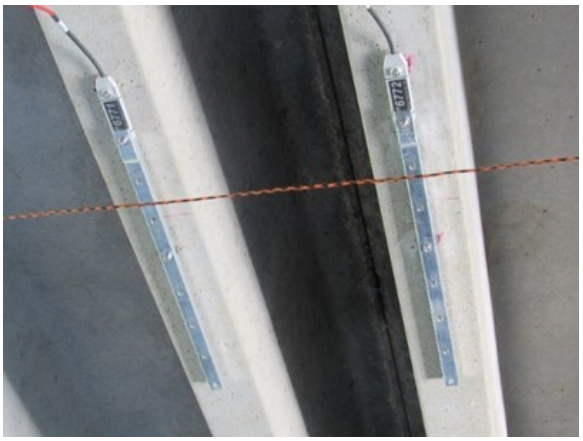

Figure 5.11 Example of strain transducers mounted at the bottom of the stems

5.3 Truck Configuration

The truck used for the field testing weighed 222 kN, with a front axle weight of 74.6 kN and a combined weight of 147.7 kN for the back two axles. The distance between the first and second axle is approximately 4.97 meters. The distance between the back two axles is about 1.5 meters. The truck used for all field tests can be seen in Figure 5.4.

(a)

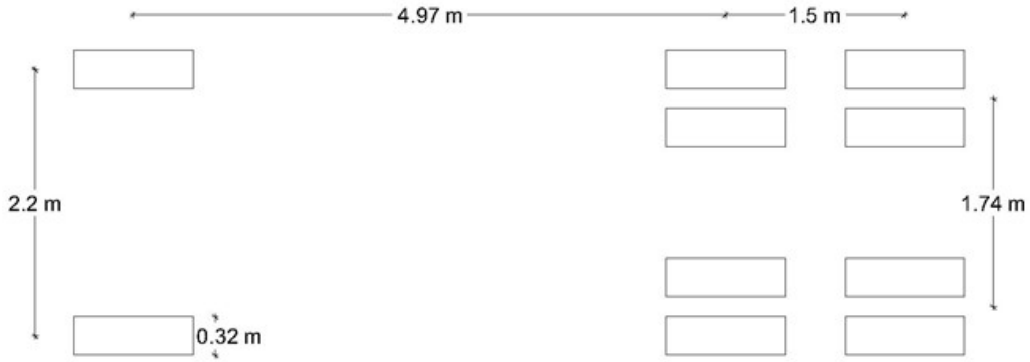

(b)

Figure 5.12 Truck used for field testing (Kidd et al. 2021): (a) side view and (b) axle configuration

6. TESTING RESULTS

6.1 Static Strain

Figure 6.1 shows the measured strains over the length of Bridge A under the static loadings. Note that the data for Path A on Bridge A were lost when transferring from the data logger. Under the Path B loading, Girder G3 exhibited the highest strain, and Girders G4 and G2, which were directly underneath the wheel paths, had the next highest strains as shown in Figure 6.1a. The strains for other girders were significantly lower since the loads were farther away from these girders. The same trend was observed for other interior load paths (see Figure 6.1b and 6.1c). Figure 6.1d shows the measured strains for Path E loading, which was on an exterior girder. It can be seen that the exterior girder had significantly larger strains than the other girders. Furthermore, Figure 6.1d shows that the three girders (G5, G6, and G7) underneath the loads had significantly higher strain values than the remaining girders. The maximum strains measured in Bridge A were in a range of 200 to 350 microstrain. Note, the highest strain was measured in Girder G7 under the Path E loading (Figure 6.1d), while the lowest strains were seen in the girders under Path D loading (Figure 6.1c).

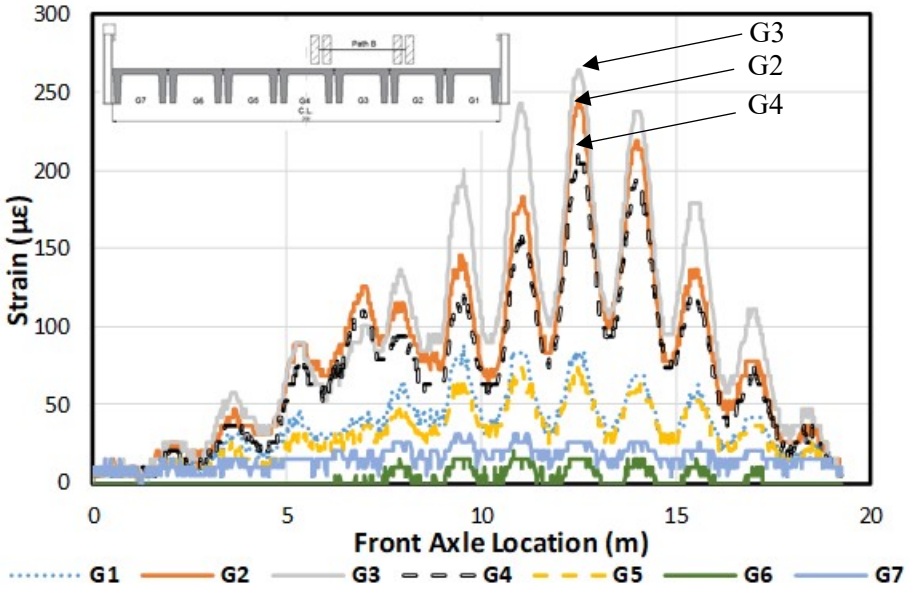

(a)

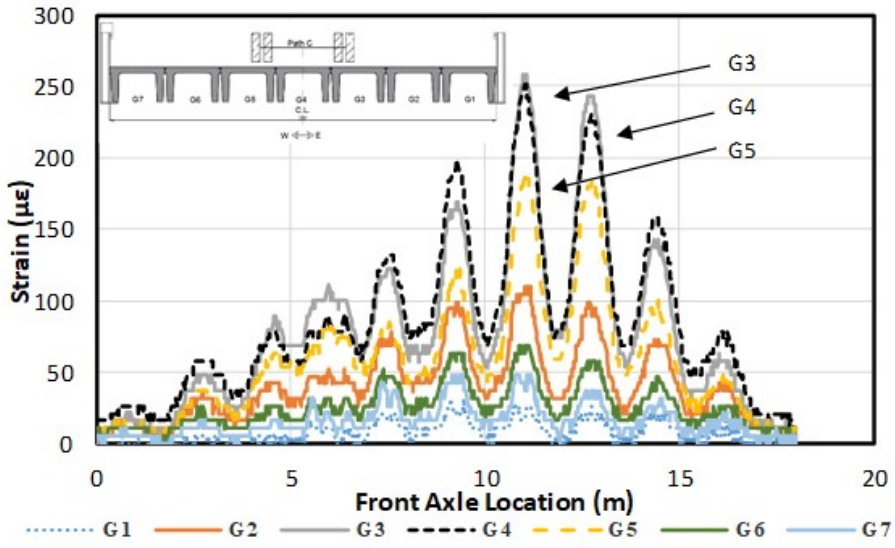
300
250
200
150
100
50
0
Strain (με)
0
5
10
15
20
Front Axle Location (m)
G3
G4
G5
G1
G2
G3
G4
G5
G6
G7

(b)

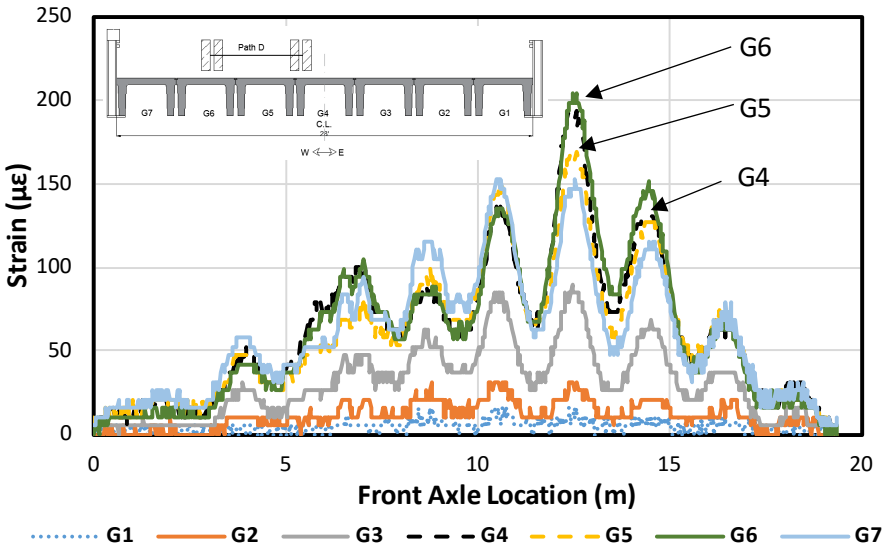
250
200
150
100
50
0
Strain (με)
0
5
10
15
20
Front Axle Location (m)
G6
G5
G4
G1
G2
G3
G4
G5
G6
G7

(c)

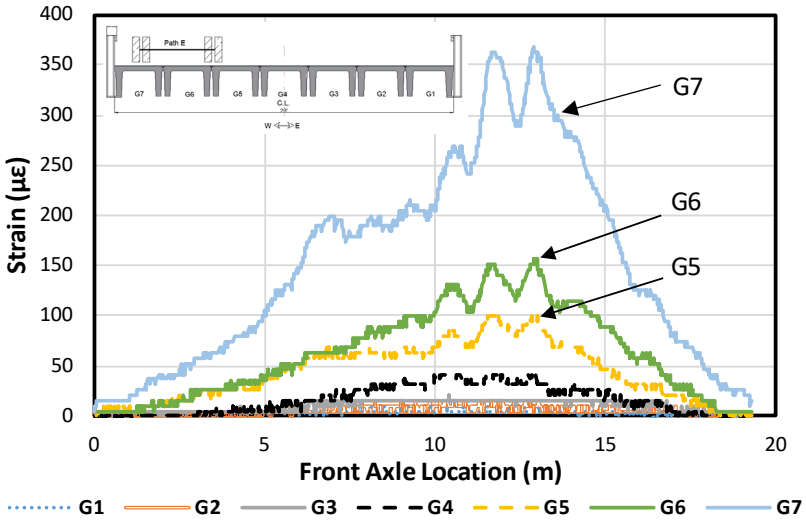

(d)

Figure 6.13 Strain versus location of the front axle of truck for Bridge A (Kidd et al. 2021): (a) Path B, (b) Path C, (c) Path D, and (d) Path E

Figures 6.2a through 6.2e show the measured strains over the length of Bridge B under the static loadings. Bridge B had strain values ranging from 600 to 1100 microstrains from the field tests. Figures 6.2a and 6.2e show the strain responses resulting in the largest strain values for the exterior girders, G1 and G8, respectively. Figure 6.2c shows the larger strain values of the girders, which were directly underneath the loads, compared with the remaining girders. A similar trend is shown in all the strain response figures for Bridge B. Meanwhile, Figure 6.2b shows that G5 has similar strain values to G3. This demonstrates that the loads were more transversely distributed across the girders directly underneath the loads than the other girders.

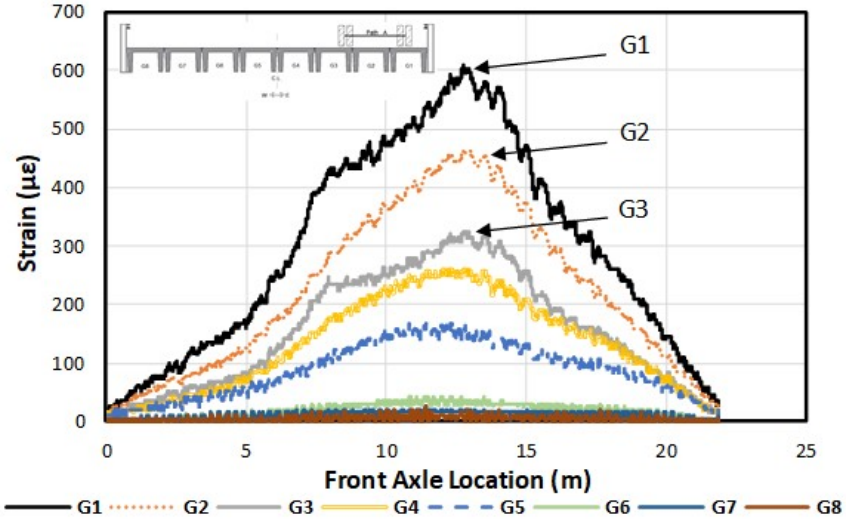

(a)

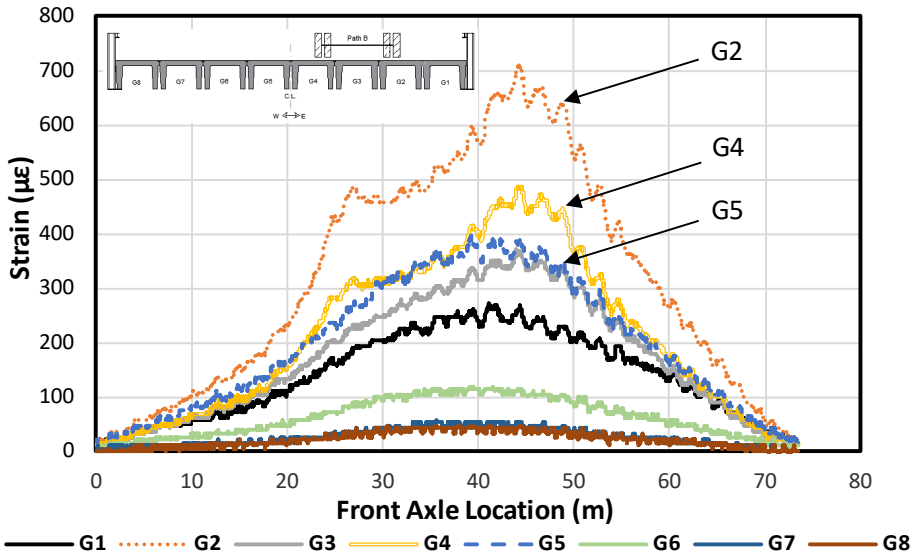
Strain (με)
Front Axle Location (m)
G2
G4
G5
G1 G2 G3 G4 G5 G6 G7 G8

(b)

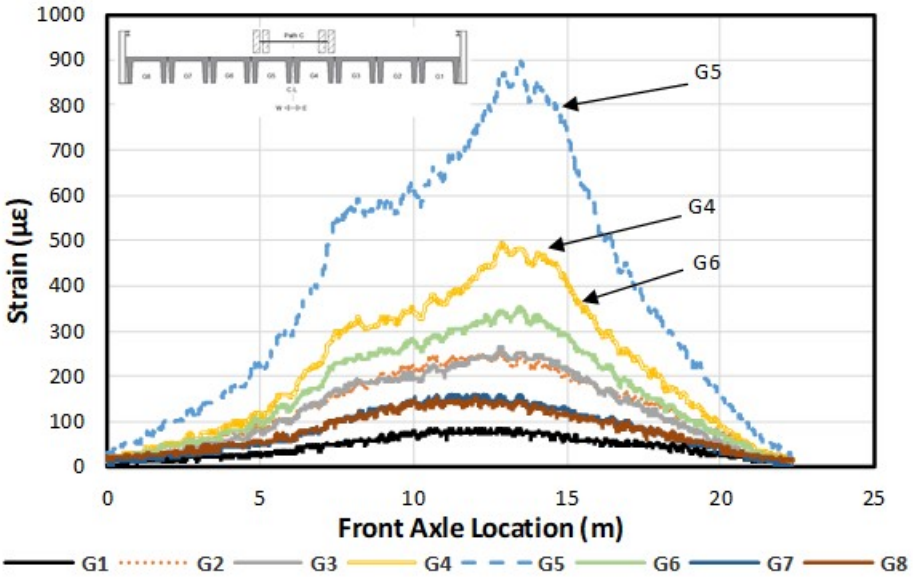
Strain (με)
Front Axle Location (m)
G5
G4
G6
G1 G2 G3 G4 G5 G6 G7 G8

(c)

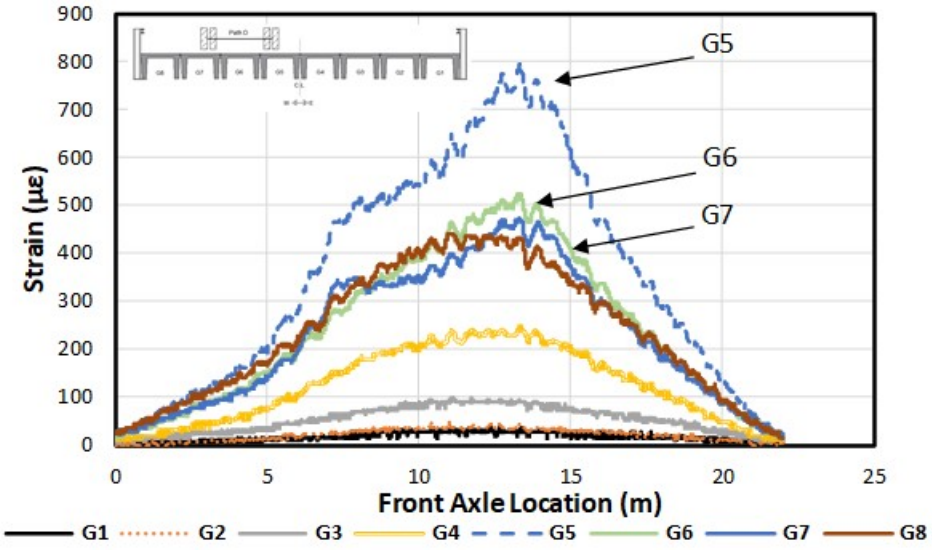

(d)

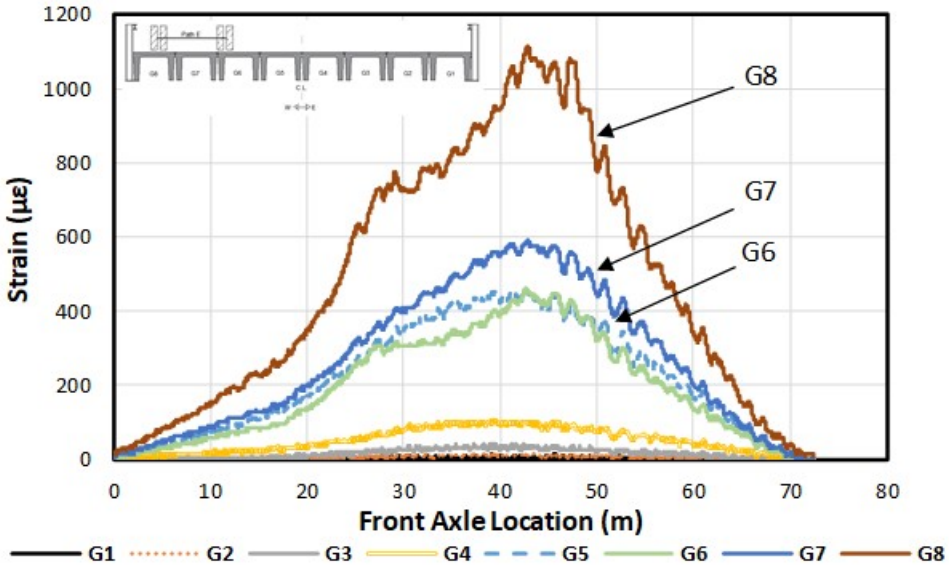

(e)

Figure 6.14 Strain versus location of the front axle of truck for Bridge B (Kidd et al. 2021): (a) Path A, (b) Path B, (c) Path C, (d) Path D, and (e) Path E

The peak strain values induced by the truck were used for the determination of the LLDFs for the girders. The average strain of the two stems for each girder was reported as the strain per girder. The field LLDFs were calculated and compared with those from AASHTO LRFD and AASHTO Standard later in Section 7.

6.2 Dynamic Strain

The goal of the dynamic tests was to determine IMs for the tested bridges. Using the strain data from both the static and dynamic tests, a strain versus truck location graph was created, comparing the strain caused by the dynamic load with the static load. Since two trials were conducted for each path, both static and dynamic, the average strain of the static field tests was compared with the average strain of the dynamic field tests. This relationship can be seen in Figures 6.3a through 6.3c for Bridge A and Figures 6.4a through 6.4c for Bridge B. The strain values from the girder with the largest maximum strain were used for these figures. As seen in these figures, the response caused by the dynamic load increased the strains when compared with the static load. However, it is noteworthy that Figured 6.3b and 6.4a show dynamic responses that are similar to the static response.

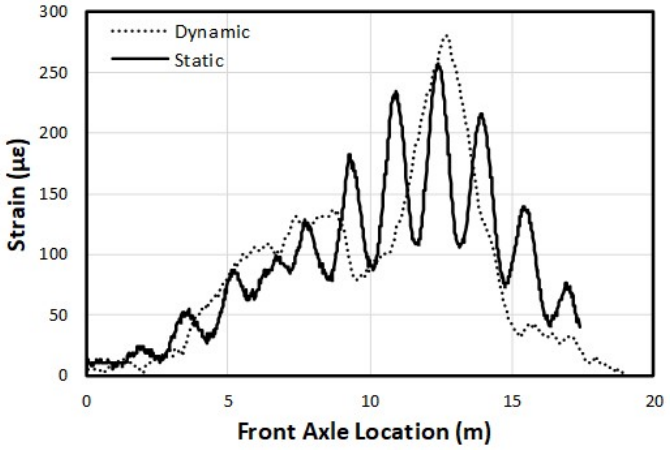

(a)

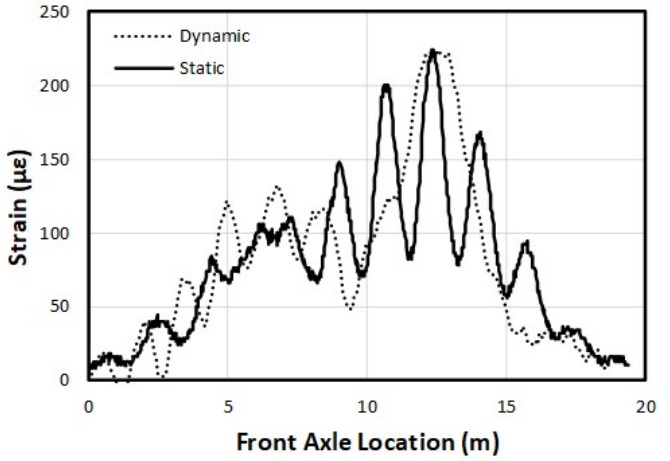

(b)

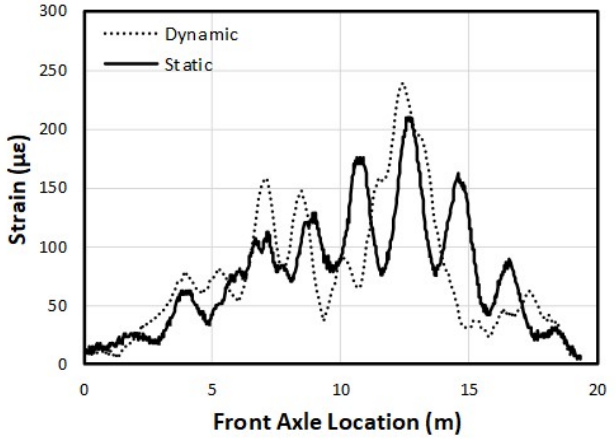

(c)

Figure 6.15 Static versus dynamic response of Bridge A: (a) Path B, (b) Path C, and (c) Path D

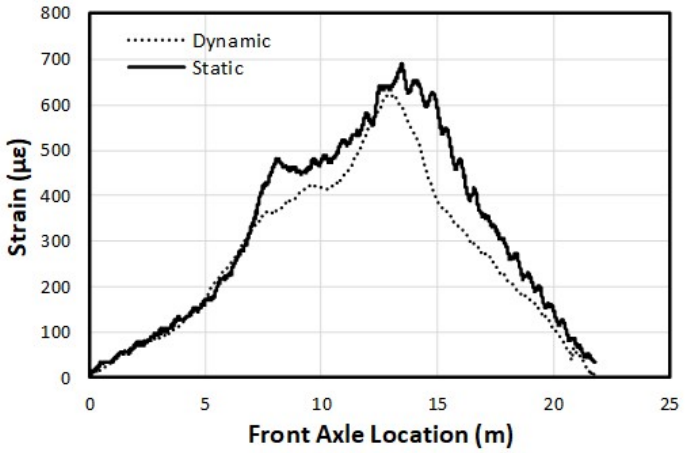

(a)

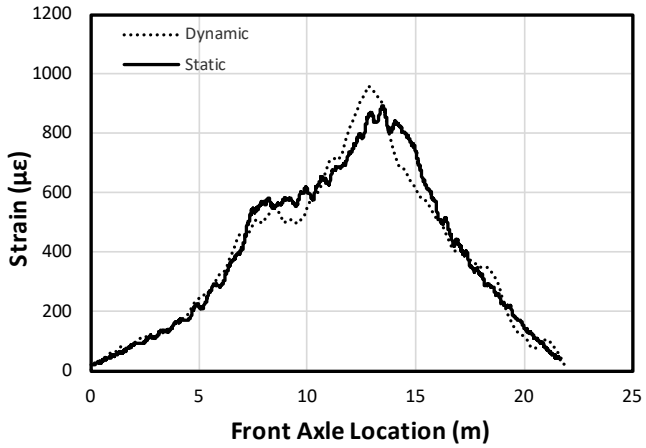

(b)

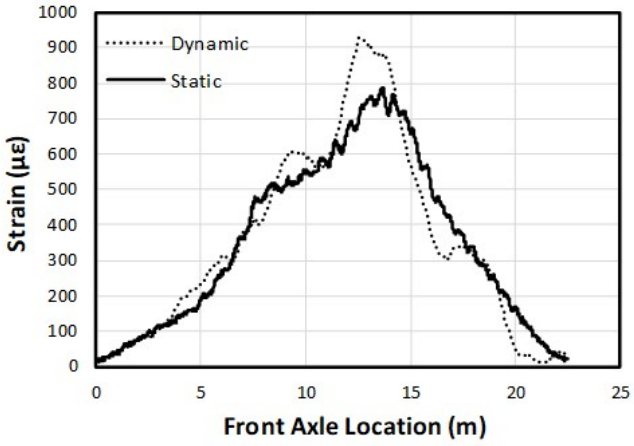

(c)

Figure 6.16 Static versus dynamic response of Bridge B: (a) Path B, (b) Path C, and (c) Path D

7. COMPARISON WITH AASHTO SPECIFICATIONS

7.1 LLDFs

The strain values from the crawl speed tests were converted into the LLDFs for both DT bridges. The commonly used equation below (Seo et al. 2014a) can be used for calculating LLDFs from the field strain.

$$LLDF = \frac{\varepsilon_i}{\sum \varepsilon_i} \quad \text{(Eq. 7.1)}$$

where ε_i is the measured strain. According to the AASHTO LRFD (AASHTO 2012), LLDFs for a DT girder can be estimated using Eq. 7.2, which was for an interior girder with one lane loaded. Note, this equation is empirical in accordance with U.S. customary units. The data were collected in U.S. customary units, therefore this equation was used.

$$LLDF_{int} = 0.06 + \left(\frac{S}{14}\right)^{0.4} \left(\frac{S}{L}\right)^{0.3} \left(\frac{K_g}{12Lt_s^3}\right)^{0.1} \quad \text{(Eq. 7.2)}$$

where S is the spacing of the girders (ft), L is the span length (ft), K_g is the longitudinal stiffness of the girder (in^4), and t_s is the thickness of the bridge deck (in) [1 ft = 0.3048 m and 1 inch = 25.4 mm]. Note, exterior girder LLDFs were calculated using the lever rule (AASHTO 2012).

According to AASHTO Standard, Eq. 7.3 through 7.6 can be used to calculate the LLDFs for both the interior and exterior girders on DTG bridges. Again, the AASHTO US version was used herein since the data were collected as such.

$$LLDF = S/D \quad \text{(Eq. 7.3)}$$

$$D = (5.75 - 0.5N_L) + 0.7N_L(1 - 0.2C)^2 \quad \text{(Eq. 7.4)}$$

$$C = K\left(\frac{W}{L}\right) \quad \text{(Eq. 7.5)}$$

$$K = [(1 + \mu)\, I/J]^{0.5} \quad \text{(Eq. 7.6)}$$

where S is the girder spacing (ft), N_L is the number of lanes, μ is the Poisson's ratio, I is the moment of inertia, J is the polar moment of inertia, W is the width of the bridge, and L is the span length of the bridge (ft). The AASHTO Standard Specifications are outdated; however, since the bridges were designed at least 30 years ago, they were designed according to the AASHTO Standard Specifications. The relation of the field LLDFs to both the AASHTO LRFD- and Standard-compliant LLDFs is necessary to be investigated. The equations above were used for all three of the approaches in terms of girder, stem, and joint because only the spacing variable changes. The following subsections explain each of the three approaches in more detail.

7.1.1 Girder Approach

This approach is the traditional way to determine LLDFs of a DT girder bridge. To find the strain per girder, the average strain value of the two stems from a single girder was calculated. While calculating the measured LLDFs, there were instances where the strain values from the gauges on the same girder did not have similar strain values. Since the stems of the same girder are nearly four feet apart transversely, the load induced on each stem will be different. Thus, taking the average of the two strains changed the strain value significantly. For Bridge A, the field LLDFs for the girder approach and AASHTO LFRD and Standard LLDFs are shown in Figures 7.1a and b for paths C and E. The percent differences for both bridges can be seen in Table 7.1. It can be seen that girder G1 has significantly larger percent differences (i.e., 144% and 160%). As mentioned before, data from path A were lost after completing the field tests; therefore, the LLDF values are outliers for this work.

The comparison shows that the AASHTO LRFD LLDFs are higher than the field LLDFs in every case except the exterior girder G7. Specifically, the AASHTO LRFD LLDFs were, on average, 34.7% larger than the field LLDFs, while the field LLDF for G7 was only higher than the AASHTO LRFD value by 2.6%. This phenomenon can be explained by the visual inspection showing that damage to the longitudinal joint is present and causes a high LLDF for G7. Meanwhile, the AASHTO Standard Specifications were significantly higher than any field LLDFs. The AASHTO Standard values were, at a minimum, 36% higher than the field LLDFs and, on average, 90% larger.

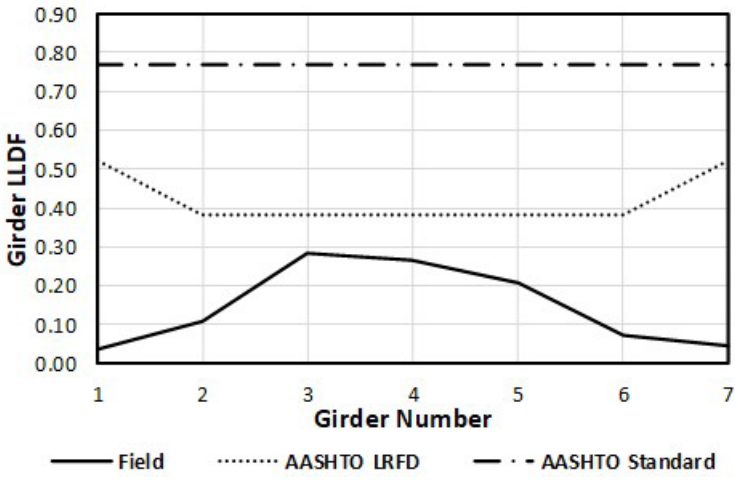

(a)

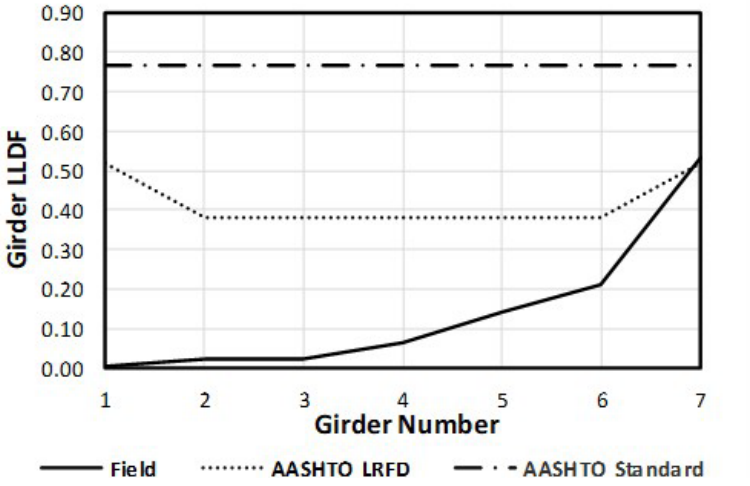

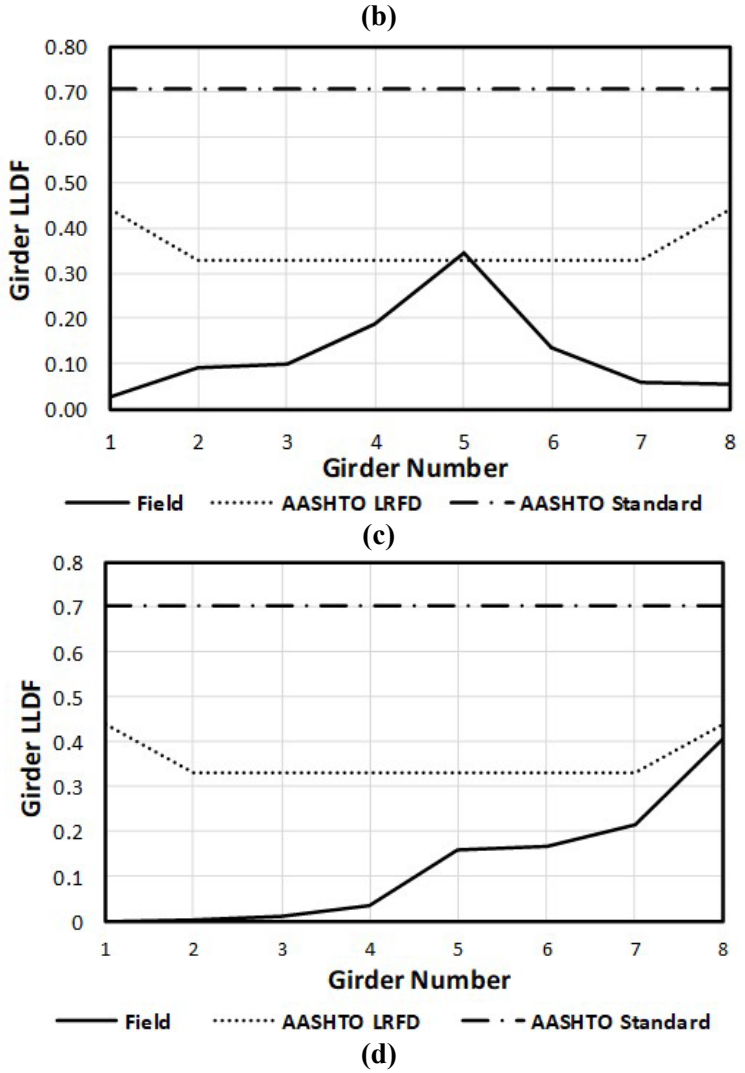

Figure 7.17 LLDFs using the girder approach (Kidd et al. 2021): (a) Bridge A – Path C, (b) Bridge A – Path E, (c) Bridge B – Path C, and (d) Bridge B – Path E

For Bridge B, the comparison can be seen in Figures 7.1c and d for paths C and E. Girder G5 has the only field LLDF that is greater than the AASHTO LRFD value. However, the field LLDF is only 2.9% larger than the AASHTO LRFD. Again, the comparison of field LLDFs and AASHTO LLDFs can be seen in Table 7.1. Leakage through the joint between G4 and G5 is believed to be the cause of this high LLDF (Kidd et al. 2021). The average percent difference between the field LLDFs and the AASHTO LRFD LLDFs is 33.3%, while the AASHTO Standard specifications significantly overestimate the field LLDFs by 91.5% on average. Again, the AASHTO Standard specifications were included in this investigation since the DT bridges are over 30 years old and were designed using the AASHTO Standard specifications.

Table 7.5 Comparison of AASHTO LLDFs to the girder approach

	Bridge A		Bridge B	
	LRFD	Standard	LRFD	Standard
Girder	Percent Difference	Percent Difference	Percent Difference	Percent Difference
G1	144.1*	160.4*	31.7	75.6
G2	34.1	95.9	14.8	83.5
G3	26.3	89.7	64.9	121.8
G4	38.9	99.7	49.3	110.5
G5	58.9	114.9	-2.9	68.4
G6	47.6	106.4	51.9	112.4
G7	-2.6	36.0	43.6	106.3
G8	-	-	7.4	53.7
Average	34.7	90.4	33.3	91.5

*Note: * means that there are no data for Path A on Bridge A and the negative percent difference indicates that field LLDFs are higher than the AASHTO values by the marked amount %.*

7.1.2 Stem Approach

With the strain values measured from the field test, Eq. 7.1 was used to calculate the LLDFs for all stems for Bridge A and B. When calculating the AASHTO LRFD and Standard values to compare with this approach, the average of the stem spacing was used in the DT girder bridge equations from the AASHTO LRFD (Eq. 7.2) and Standard (Eq. 7.3), respectively. It should be noted that the LLDFs of the stems on the exterior girders were calculated using the lever rule for the AASHTO LRFD specifications. The reaction of the two stems was found using the lever rule, and a multiple presence factor of 1.2 was applied to both stems.

Figures 7.2a and 7.2b for paths C and E compare the LLDFs by stem to the AASHTO LLDF values for Bridge A. Stem 13, which is the inside stem of the exterior girder, has a substantially higher LLDF than the AASHTO LRFD LLDF value. Besides, Stem 13, the rest of the field LLDFs were lower than the AASHTO LRFD values. The percent differences for the stem approach can be seen in Table 7.2. Specifically, Stem 13 has a value 7.5% higher than the AASHTO Standard LLDF. It should be noted that Stem 13 on Bridge A is the only time the field LLDF exceeded the codified LLDFs from the AASHTO Standard specifications. Stem 12 has a noticeably smaller value than Stem 13; the two stems are separated by only a joint. This is another indicator of joint damage at that location. Path A data were lost when transferring the data between the data logger and computer; therefore, the field LLDFs of Stem 1 and 2 did not show a similar trend to the other exterior stems. As shown in Table 7.2, the average of all the percent differences of the stem approach was also calculated. The AASHTO LRFD and AASHTO Standard have average percent differences from the field LLDFs of 55.5% and 81.6%, individually.

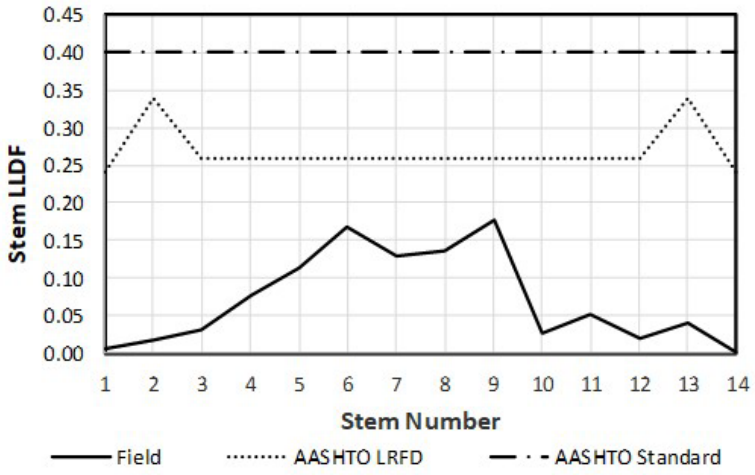
0.45
0.40
0.35
0.30
0.25
0.20
0.15
0.10
0.05
0.00
Stem LLDF
1 2 3 4 5 6 7 8 9 10 11 12 13 14
Stem Number
Field
AASHTO LRFD
AASHTO Standard

(a)

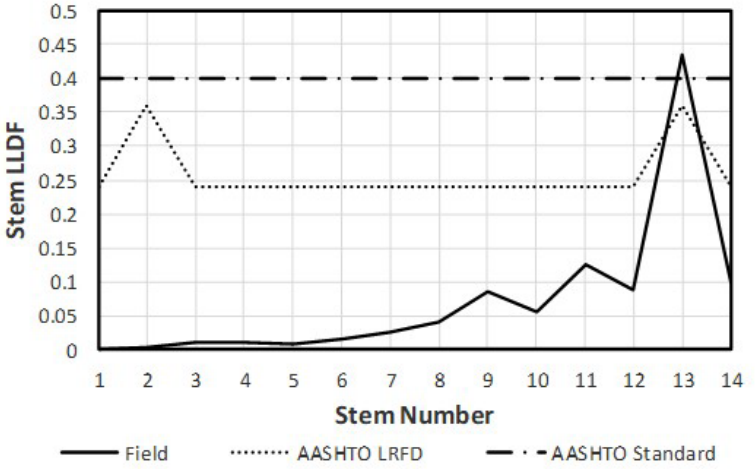
0.5
0.45
0.4
0.35
0.3
0.25
0.2
0.15
0.1
0.05
0
Stem LLDF
1 2 3 4 5 6 7 8 9 10 11 12 13 14
Stem Number
Field
AASHTO LRFD
AASHTO Standard

(b)

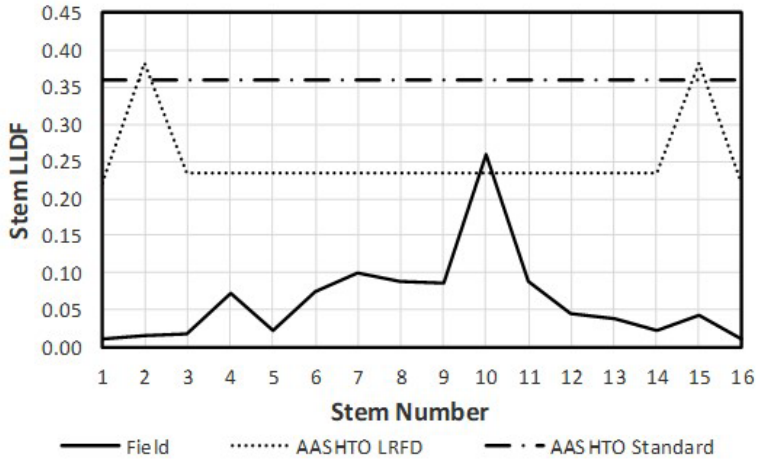
0.45
0.40
0.35
0.30
0.25
0.20
0.15
0.10
0.05
0.00
Stem LLDF
1 2 3 4 5 6 7 8 9 10 11 12 13 14 15 16
Stem Number
Field
AASHTO LRFD
AASHTO Standard

(c)

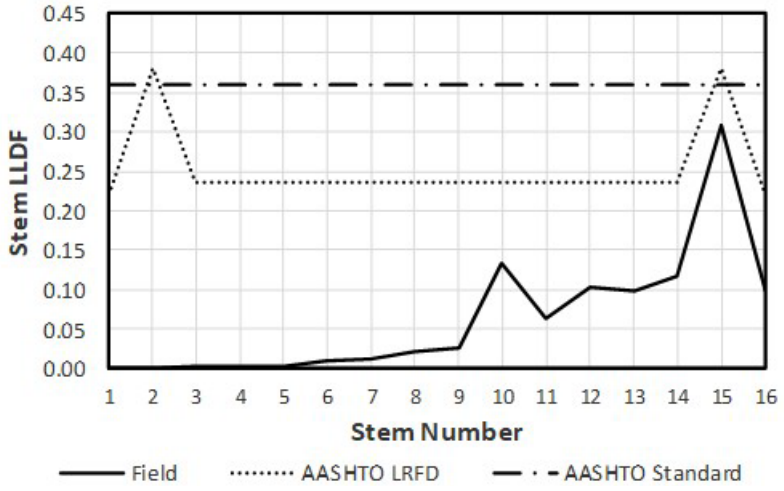

(d)

Figure 7.18 LLDFs using the stem approach: (a) Bridge A – Path C, (b) Bridge A – Path E, (c) Bridge B – Path C, and (d) Bridge B – Path E

Table 7.6 Comparison of AASHTO LLDFs to the stem approach

Stem	Bridge A		Bridge B	
	LRFD	Standard	LRFD	Standard
	Percent Difference	Percent Difference	Percent Difference	Percent Difference
S1	167.3*	178.2*	32.7	79.4
S2	138.7*	147.3*	81.2	76.9
S3	89.7	121.1	55.3	94.3
S4	41.3	80.8	-1.5	43.4
S5	57.6	94.9	83.5	117.4
S6	42.5	81.9	78.6	113.5
S7	54.7	92.4	64.4	101.9
S8	63.2	99.5	88.9	121.7
S9	37.4	77.4	90.2	122.6
S10	129.8	151.7	-11.8	33.5
S11	47.2	86.0	88.4	121.3
S12	99.0	128.5	70.0	106.5
S13	-25.0	-7.5	69.3	105.9
S14	89.8	121.0	65.6	102.9
S15	-	-	21.7	16.6
S16	-	-	74.8	114.1
Average	55.5	81.6	61.1	92.0

*Note: * means Bridge A does not have data for S1 and S2, and the negative percent difference indicates that field LLDFs are higher than the AASHTO values by the marked amount %.*

Figures 7.2c and 7.2d compare the field LLDFs from Bridge B with the two AASHTO design codes for paths C and E. The percent differences for Bridge B can be seen in Table 7.2. Stem 10 has a field LLDF higher than the AASHTO LRFD value by 11.8%, showing similar results to the girder approach.

However, now there is another LLDF value greater than the AASHTO LRFD values. Stem 4 is now 1.5% larger than the AASHTO LRFD design value, although the AASHTO Standard value is larger than the field LLDF. Interestingly, the significant difference in LLDFs between adjacent stems, S4 and S5, may suggest joint damage on the joint between G2 and G3.

7.1.3 Joint Approach

Because the strain values in stems on the same girder were not similar, LLDFs for the stems on either side of the same joint were investigated. The field LLDFs were calculated by taking the average of two stems on a joint, but the exterior stems were not averaged with another value. The AASHTO LRFD equation used the spacing between the longitudinal joints, which is the overall width of the girder.

The comparison between the field LLDFs and the two AASHTO-compliant values for Bridge A can be seen in Figures 7.3a and 7.3b for paths C and E. Table 7.3 shows the percent difference of the field LLDFs compared with the two AASHTO values for Bridges A and B using the joint approach. Joint 7 on Bridge A, including stems 12 and 13, has the only LLDF higher than the AASHTO LRFD value by 22%. This is comparable to the result from the stem approach, but the LLDF is higher in the joint approach. It should be noted that the girder LLDF still yielded the highest value. The AASHTO Standard value is higher than all the field LLDFs by an average of 107.2%.

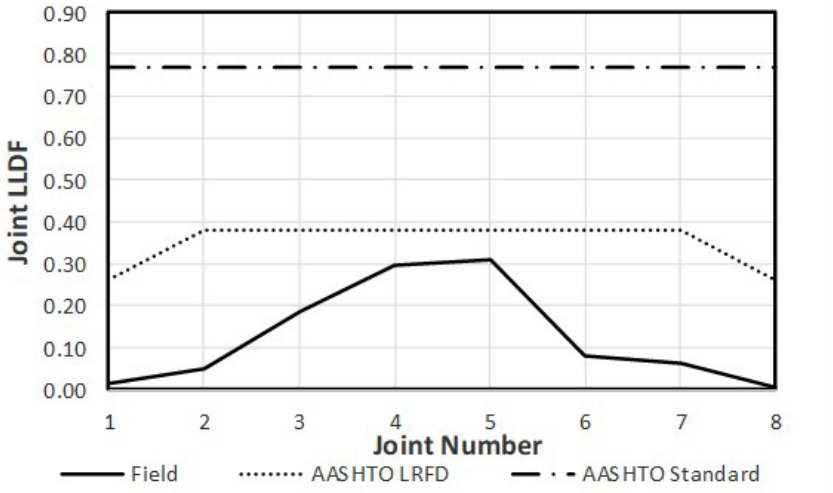

(a)

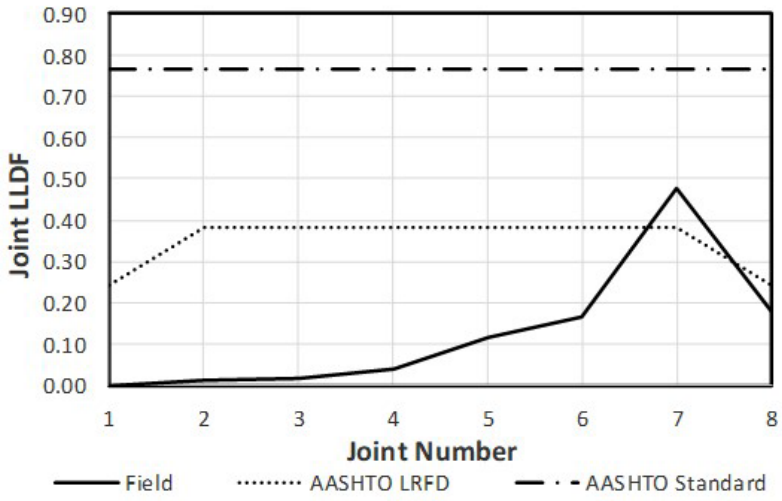
0.90
0.80
0.70
0.60
0.50
0.40
0.30
0.20
0.10
0.00
Joint LLDF
1
2
3
4
5
6
7
8
Joint Number
Field
AASHTO LRFD
AASHTO Standard

(b)

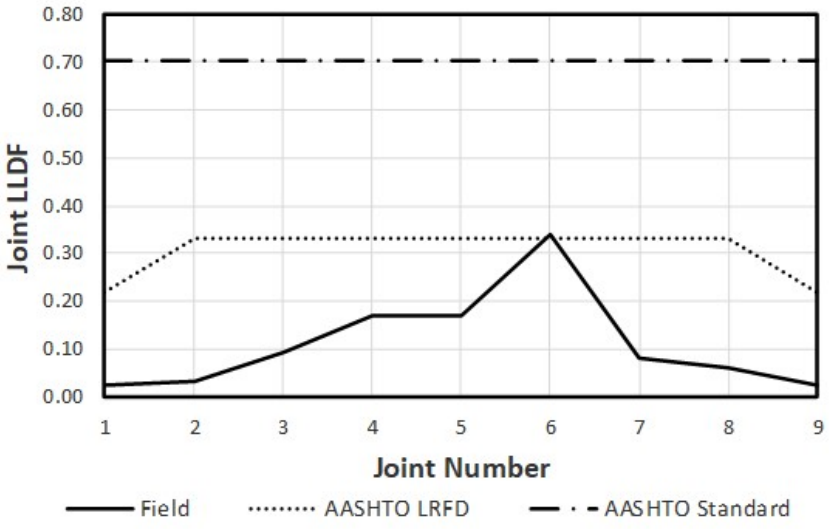
0.80
0.70
0.60
0.50
0.40
0.30
0.20
0.10
0.00
Joint LLDF
1
2
3
4
5
6
7
8
9
Joint Number
Field
AASHTO LRFD
AASHTO Standard

(c)

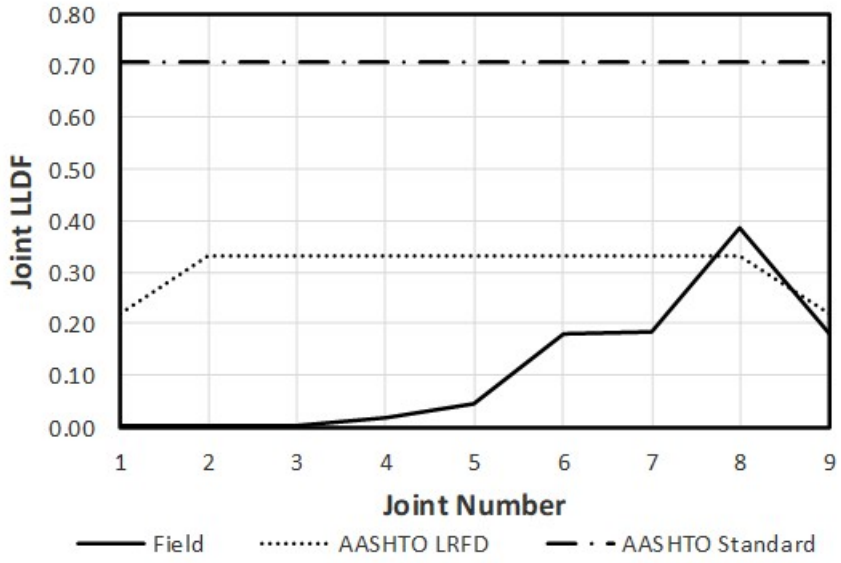

(d)

Figure 7.19 LLDFs using the joint approach: (a) Bridge A – Path C, (b) Bridge A – Path E, (c) Bridge B – Path C, and (d) Bridge B – Path E

The joint approach data are different from the girder approach for Bridge B, as seen in Figure 7.3c and 7.3d for path C and E. As shown in Table 7.3, the joint J6, between G5 and G6, has the LLDF higher than the AASHTO LRFD value by 1%. However, joint J8 and J1 now have a value higher than the AASHTO LRFD value. The girder approach showed that the exterior girder, G8, did not have a field LLDF higher than the AASHTO LRFD value. Joint 8, which is the interior stem of G8, now exceeded the AASHTO LRFD value by 13.6% when using the joint approach. Joint J1 exceeded the AASHTO LRFD value by 21.6%. The AASHTO Standard value is higher than all the field LLDFs by an average of 95.2%. The AASHTO LRFD code is, on average, 28.9% higher than field LLDFs.

Table 7.7 Comparison of AASHTO LLDFs to the joint approach

	Bridge A		Bridge B	
	LRFD	Standard	LRFD	Standard
Joint	Percent Difference	Percent Difference	Percent Difference	Percent Difference
J1	141.0*	177.8*	-21.6	89.0
J2	84.0*	132.6*	28.6	94.7
J3	21.9	86.1	20.4	88.1
J4	25.3	88.9	47.2	109.0
J5	20.4	84.8	64.9	121.8
J6	60.8	116.3	-1.0	70.0
J7	-22.0	47.1	44.1	106.7
J8	36.4	123.9	-13.6	58.7
J9	-	-	18.8	118.5
Average	38.7	107.2	28.9	95.2

*Note: * means there are insufficient data for J1 and J2, and the negative percent difference indicates that field LLDFs are higher than the AASHTO values by the marked amount %.*

7.1.4 Comparison of Three Approaches

The three different approaches of calculating the field LLDFs were compared with the AASHTO LRFD and the AASHTO Standard values using percent differences. The percent differences for the girder, stem, and joint approaches are shown in their respective tables (see Tables 7.1 through 7.3). The average of the percent differences was also calculated and used to compare the three different approaches as listed in Table 7.4. Since Path A for Bridge A did not have data, the field LLDF values are not representative of the LLDF. Hence, the corresponding percent difference values were not included when calculating the average percent difference of each approach.

Table 7.8 Average percent differences of three approaches

	Bridge A		Bridge B	
Percent Difference	AASHTO LRFD	AASHTO Standard	AASHTO LRFD	AASHTO Standard
Girder	34.7	90.4	33.3	91.5
Stem	55.5	81.6	61.1	92.0
Joint	38.7	107.2	28.9	95.2

The average percent differences are shown for both the AASHTO LRFD and the AASTHO Standard specifications. The AASHTO LRFD values are much closer to the field LLDFs, but the AASHTO Standard values are not similar to those from the field testing. If the two trials of each approach for Bridge A and Bridge B are averaged, the joint and girder approaches are nearly identical at 33.8% and 34%, respectively. However, the stem approach is significantly higher, at 58.3%, than the joint and girder approaches. Therefore, the stem approach is more conservative than the other two approaches, according to the percent differences.

Meanwhile, the stem approach also has a similar pattern to the field LLDFs, specifically when determining the stems on the exterior girders. The LLDF of the stem on the inside of the exterior girder is larger than the LLDF of the outer stem of the exterior girder, and it is also larger than the LLDF of the stems on the interior girders. The joint approach also has higher LLDFs for the interior joint of the exterior girder than it does for the exterior joint of the exterior girder. The difference between the stem and joint approaches is that the interior LLDFs are higher than the exterior LLDFs for the joint approach. In the stem approach, that is not the case.

7.2 IM

The goal of the dynamic tests was to determine IM values for the DT bridges. From the data collected during the field tests, the IM values were calculated using Eq 7.7. The data from both the static tests and dynamic tests were used in Eq. 7.7.

$$IM = \frac{R_D - R_S}{R_S} * 100 \quad \text{(Eq. 7.7)}$$

where R_d (με) is the response from the dynamic test and R_S (με) is the response from the static test. The AASHTO Standard specifications uses Eq. 7.8 to calculate the IM values for both bridges. These equations are based on imperial units.

$$IM = \frac{50}{L+125} \leq 0.3 \quad \text{(Eq. 7.8)}$$

The IM values were calculated from the strain graphs in Figures 6.3 and 6.4 and presented in Table 7.5. The max IM value from the field tests is from Bridge A at 14.4%. This value is lower than the AASHTO LRFD value by 56% and lower than the AASHTO Standard value by 52%.

Table 7.9 Comparison of measured and specified dynamic load allowance (IM, %)

	Bridge A			Bridge B		
Test	**Measured**	**AASHTO LRFD**	**AASHTO Standard**	**Measured**	**AASHTO LRFD**	**AASHTO Standard**
Path B	8.4	33	29.9	0	33	28.6
Path C	0	33	29.9	7.1	33	28.6
Path D	14.4	33	29.9	8.9	33	28.6

The IM values are, on average, higher for Bridge A than Bridge B. Considering that Bridge B has a larger span length, the results generally agreed with other studies relating the span length to IM. It should also be noted that Path D caused the largest IM value on Bridge A. Path D loaded the same joint that caused G7 to have the LLDF that exceeded the AASHTO LRFD design value. Figures 3.3 and 3.6 provide examples of the damage at the joints where the research team believes damage affected the outcome of the test. A similar trend occurred during the field tests on Bridge B. Path D had the largest IM and it loaded G5, which had the LLDF value larger than the AASHTO LRFD value.

8. ANALYTICAL STUDY

8.1 Computational Modeling

The field tests proved that the AASHTO LRFD specifications are generally conservative for the two tested DT bridges (Bridges A and B) unless sufficient damage is present. However, more data are necessary to determine if this is correct for the majority of DT girders in service. To study this, computational models were made of Bridges A and B, and they were calibrated to accurately represent the conditions of each. The models were created in CSi Bridge, which has already been proven to accurately depict the response of a bridge due to a moving load (Torres 2016; Huang and Davis 2018). The models were made using solid elements for the stems of the DT girder, and shell elements were used for the flanges. Two-joint link elements were used to connect the stems to the flanges to make one composite DT girder. To connect the adjacent DT girders, two-joint links were used between the DT girder flanges (shell elements). Pin restraints were applied at the bottom of each stem at the ends of the DT girders to represent the abutment. The models for Bridges A and B can be illustrated in Figure 8.1a and 8.1b.

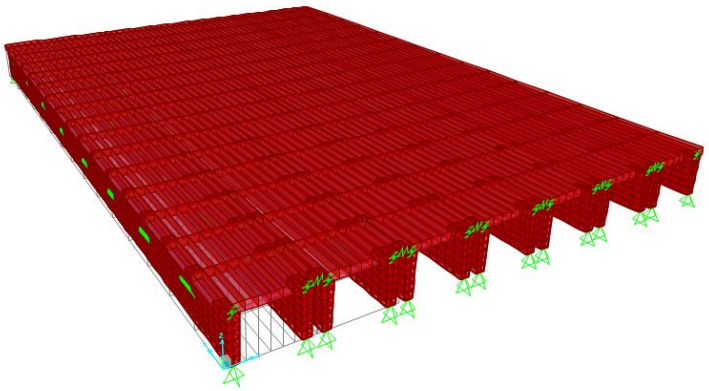

(a)

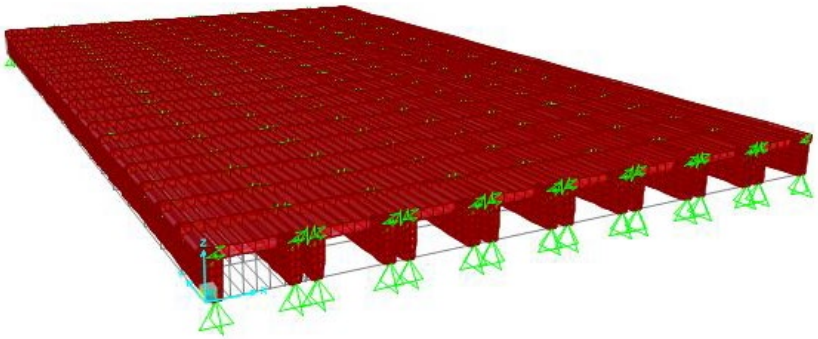

(b)

Figure 8.20 Analytical models developed in CSi Bridge: (a) Bridge A and (b) Bridge B

8.2 Calibration with Field Data

Once the model was created using the bridge plans, the models needed to be calibrated. The DT bridges were 34 and 38 years old, respectively, and had significant instances of damage. To account for this damage and calibrate the model with the field strain data, multiple changes to the models were made. Both bridges were calibrated with the data from Path C of the respective field tests because most traffic is down the center of the bridge, similar to Path C. The shear stiffness of the two-joint links between the DT girders was modified to represent the damage of the longitudinal joints. Since the bridges have been in service for over 30 years, cracking in the DT girders can be expected. Thus, a reduction factor was applied to the modulus of elasticity of the concrete. For Bridge A, the modulus of elasticity of the concrete in the flanges of the DT girder was not reduced. However, the concrete in the flanges for Bridge B required a reduction in modulus of elasticity. Bridge B has a smaller cross-sectional depth and a longer span length than Bridge A. Hence, more cracking would be prevalent in Bridge B. Bridge B also required another reduction since there was shear cracking in girder G4. G4 was the only girder that received this reduction.

The analytical model was compared with the field data by percent differences. The equation for percent difference is shown in Eq. 8.1.

$$\text{Percent Difference } (\%) = \left(\frac{\text{Analytical} - \text{Field}}{\frac{\text{Analytical} + \text{Field}}{2}} \right) * 100 \qquad \text{(Eq. 8.1)}$$

Table 8.1 shows the comparison of the analytical LLDFs to the field LLDFs of Bridge A. The percent differences of the analytical and field LLDFs are within 10% for most of the girders, which are directly loaded with the truck. The two exceptions are the girders with low LLDFs. The nature of the percent difference function exaggerates the difference of the two values, even though the analytical LLDFs are only different by less than two-hundredths.

Table 8.10 Calibration of LLDFs for Bridge A

	G1	G2	G3	G4	G5	G6	G7
Analytical	0.037	0.101	0.257	0.252	0.225	0.092	0.035
Field	0.035	0.108	0.281	0.264	0.205	0.073	0.044
Percent Difference	5.98	6.73	9.02	4.79	9.49	23.22	22.65

The comparison of the analytical LLDFs to the field LLDFs of Bridge B is shown in Table 8.2. Again, the percent differences of the exterior girders are large because the numbers are extremely small. The girders that are underneath the truck load have percent differences of only less than 10%.

Table 8.11 Calibration of LLDFs for Bridge B

	G1	G2	G3	G4	G5	G6	G7	G8
Analytical	0.063	0.088	0.104	0.199	0.314	0.137	0.062	0.032
Field	0.028	0.09	0.098	0.189	0.345	0.136	0.059	0.055
Percent Difference	77.12	1.93	6.35	5.01	9.34	0.59	5.13	52.00

8.3 Parametric Study

The calibrated models were then used to conduct a parametric study. The cost and time to study the LLDFS of DT girder bridges with many different geometries and variables using field tests are substantial. Therefore, the calibrated models were modified to represent a variety of different DT bridges. The parameters that were modified during this study include span length, location of diaphragms, deck width, concrete strength, and width-length ratio. The basis for determining the ranges of the parameters' values was based upon the current DT bridges in South Dakota since these two cross-sections are standard for South Dakota bridges. For example, according to the South Dakota Department of Transportation's bridge management system, the shortest and longest span of a single span DT girder bridge is 6.1 meters and 30.5 meters, respectively. Each model created was tested over the same paths as the field tests. Hence, each model had five paths. The exceptions include when the deck width of the bridge was altered. Paths were added when the deck width was increased, and paths were removed when the deck width decreased.

8.3.1 Span Length

As mentioned above, the span length of the DT girder bridges was investigated between 6.1 and 30.5 meters. The change in LLDFs as a function of span length for Bridge A is shown in Figures 8.2a and 8.2b for interior and exterior girders, correspondingly. Corresponding values are shown in Table 8.3. The analytical interior LLDFs decrease at a rate of 10.8% as the span length increases by 6.1 meters, on average. As seen in Figure 8.2, the AASHTO LRFD LLDFs match the pattern of the analytical LLDFs and are conservative. The percent difference varies from 25.7% to 15.8% as the span length increases. The AASHTO LRFD exterior LLDFs, however, do not show the same trend as the analytical LLDFs since the lever rule does not account for span length. At a span length of 30.5 meters, the percent difference is 57.7%. This is overly conservative. The exterior analytical LLDFs decrease at an average rate of 8.1% due to the increase by 6.1 meters. As expected, the AASHTO Standard is significantly higher than the analytical LLDFs and AASHTO LRFD LLDFs in all instances.

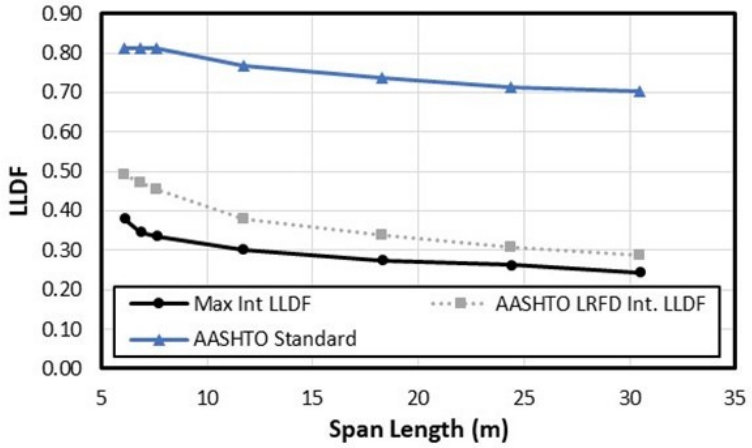

(a)

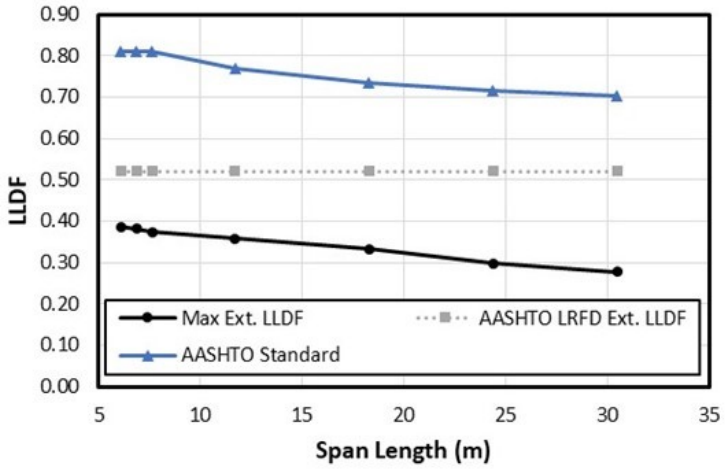

(b)

Figure 8.21 Change in LLDFs due to span length in Bridge A: (a) interior LLDFs and (b) exterior LLDFs

Table 8.12 Change in LLDF due to span length in Bridge A: (a) interior LLDFs and (b) exterior LLDFs

(a)

Span (m)	Max Int. LLDF	AASHTO LRFD Int. LLDF	AASHTO Standard LLDF
6.1	0.380	0.492	0.811
6.86	0.347	0.472	0.811
7.62	0.336	0.455	0.811
11.7	0.303	0.380	0.768
18.3	0.275	0.338	0.736
24.4	0.262	0.308	0.715
30.5	0.245	0.287	0.703

(b)

Span (m)	Max Ext. LLDF	AASHTO LRFD Ext. LLDF	AASHTO Standard LLDF
6.1	0.386	0.520	0.811
6.86	0.381	0.520	0.811
7.62	0.374	0.520	0.811
11.7	0.358	0.520	0.768
18.3	0.333	0.520	0.736
24.4	0.297	0.520	0.715
30.5	0.278	0.520	0.703

The change in LLDFs due to the change in span length for Bridge B is shown in Figures 8.3a and 8.3b for interior and exterior girders, separately. The analytical and two AASHTO design values are shown in Table 8.4. The analytical interior LLDFs in Figure 8.3 are almost identical to the AASHTO LRFD until the span length is less than or equal to 12.2 meters. The analytical interior LLDFs are then slightly greater than the AASHTO LRFD values. However, this is due to the shear crack in girder G4. G4 cannot resist the load at Path C, which transfers more load to G5. In the analytical study, G5 had the only interior LLDFs that exceed the AASHTO LRFD LLDFs. The interior analytical LLDFs decrease by 8.5% due to the increase by 6.1 meters on average. Similar to Bridge A, the exterior AASHTO LRFD LLDFs do not match the pattern of the analytical LLDFs. However, the AASHTO LRFD exterior LLDFs are more accurate; at a span length of 30.5 meters, the percent difference is 40%. At a span length of 6.1 meters, the exterior LLDF barely exceeds the AASHTO LRFD LLDFs. The AASHTO Standard LLDFs continue to be significantly higher. It is important to notice that the analytical exterior LLDFs decrease with span length, even when it is not considered when calculating AASHTO LRFD exterior LLDFs.

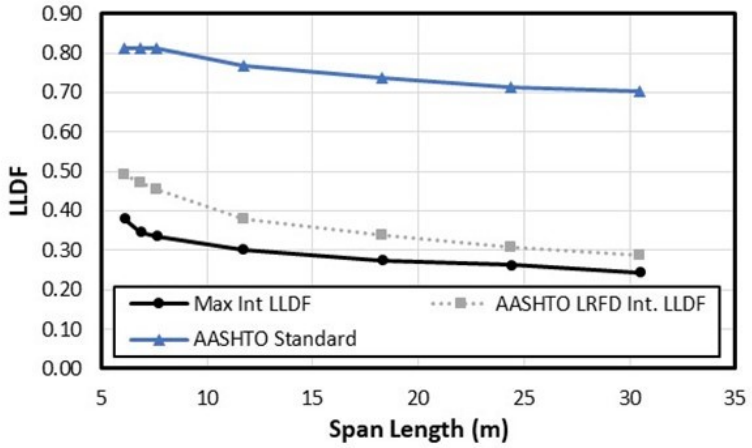

(a)

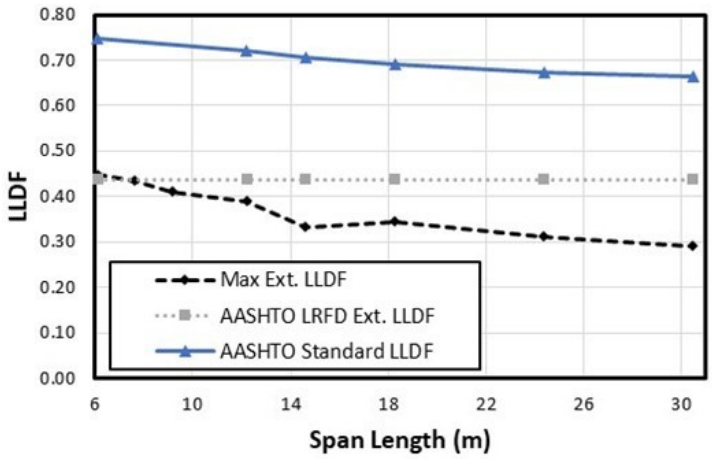

(b)

Figure 8.22 Change in LLDFs due to span length in Bridge B: (a) interior LLDFs and (b) exterior LLDFs

Table 8.13 Change in LLDFs due to span length in Bridge B: (a) interior LLDFs and (b) exterior LLDFs

(a)

Span (m)	Max Int. LLDF	AASHTO LRFD Int. LLDF	AASHTO Standard LLDF
6.1	0.540	0.447	0.747
7.62	0.488	0.414	0.747
9.14	0.447	0.389	0.747
12.2	0.363	0.353	0.721
14.6	0.314	0.330	0.705
18.3	0.307	0.309	0.69
24.4	0.285	0.282	0.674
30.5	0.259	0.263	0.664

(b)

Span (m)	Max Ext. LLDF	AASHTO LRFD Ext. LLDF	AASHTO Standard LLDF
6.1	0.448	0.438	0.747
7.62	0.435	0.438	0.747
9.14	0.411	0.438	0.747
12.2	0.391	0.438	0.721
14.6	0.327	0.438	0.705
18.3	0.345	0.438	0.69
24.4	0.312	0.438	0.674
30.5	0.292	0.438	0.664

8.3.2 Location of Diaphragms

The location of the diaphragms was varied between no diaphragms, at the endspans, at the midspan, and both the midspan and endspan. The variation in interior and exterior LLDFs based on the location of diaphragms on Bridge A is shown in Figure 8.4a and 8.4b. The data corresponding to Figure 8.4 can be seen in Table 8.5. There is no significant change (≤2%) in maximum LLDFs when diaphragms at the endspan are present. When diaphragms are present at both endspan and midspan, interior LLDFs increase and exterior LLDFs decrease. Again, this value is very minimal. It shows yet again that AASHTO LRFD LLDFs may be too conservative for exterior LLDFs.

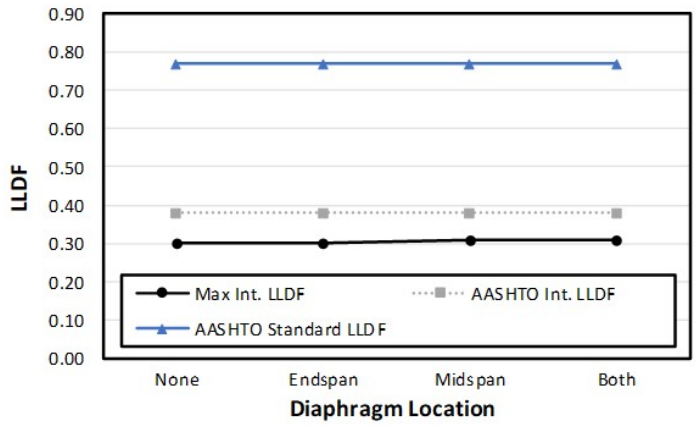

(a)

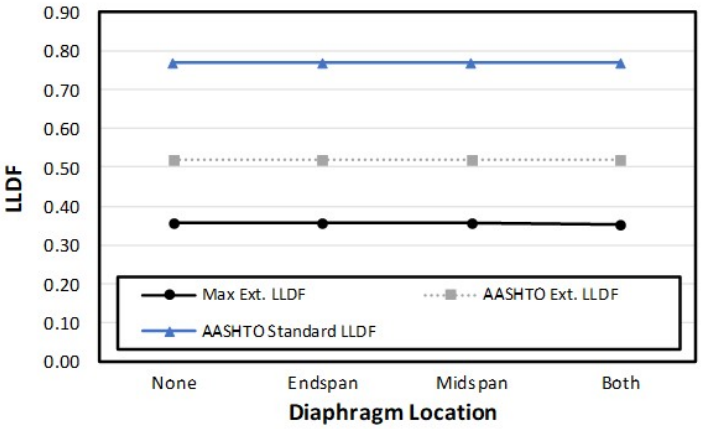

(b)

Figure 8.23 Change in LLDFs due to diaphragm location in Bridge A: (a) interior LLDFs and (b) exterior LLDFs

Table 8.14 Change in LLDFs due to diaphragm location in Bridge A: (a) interior LLDFs and (b) exterior LLDFs

(a)

Diaphragm Location	Max Int. LLDF	AASHTO LRFD Int. LLDF	AASHTO Standard LLDF
None	0.314	0.33	0.705
Endspan	0.318	0.33	0.705
Midspan	0.319	0.33	0.705
Both	0.298	0.33	0.705

(b)

Diaphragm Location	Max Ext. LLDF	AASHTO Ext. LLDF	AASHTO Standard LLDF
None	0.358	0.52	0.768
Endspan	0.358	0.52	0.768
Midspan	0.356	0.52	0.768
Both	0.353	0.52	0.768

The same analysis was done on Bridge B, as seen in Figures 8.5a and 8.5b for interior and exterior girders and Table 8.6. When diaphragms are present at the midspan and endspan, both the LLDFs decrease. Otherwise, there is very little change (6% max) in LLDFs. The presence of diaphragms at the midspan and endspan changed the LLDFs by a maximum of 15% and 5% on average. Since this was not as obvious in Bridge A, it suggests that a 584-mm-deep DT girder cannot fully transfer the load like a 762-mm-deep girder when it is damaged. Similar to the trend in LLDFs due to the increase in the span length, the AASHTO Standard LLDFs appear to be much higher than those from the parametric study.

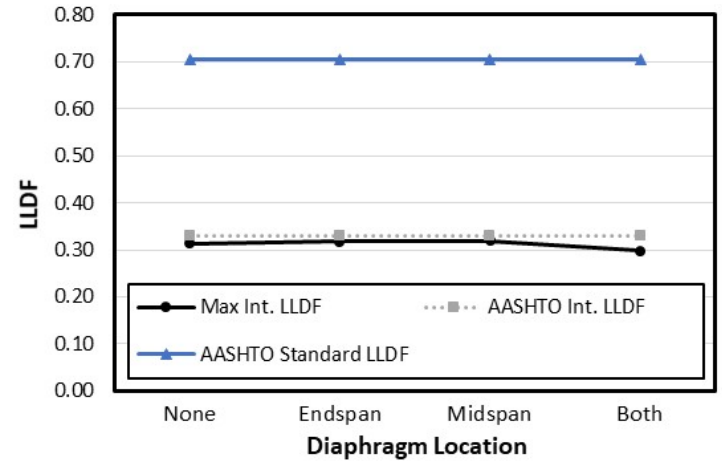

(a)

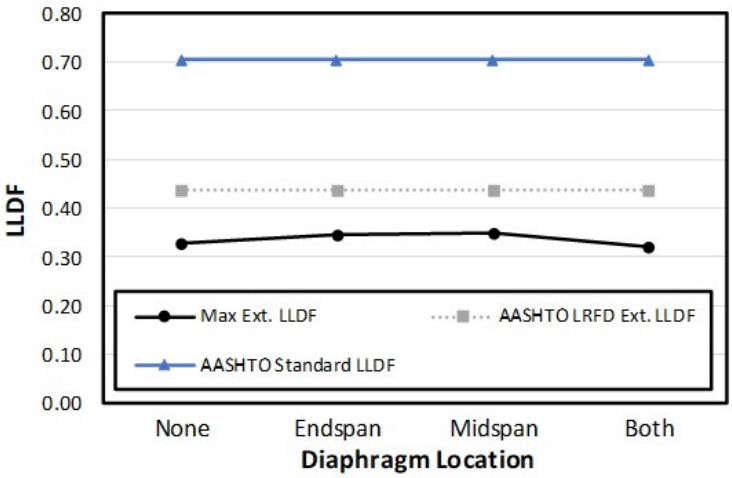

(b)

Figure 8.24 Change in LLDFs due to diaphragm location in Bridge B: (a) interior LLDFs and (b) exterior LLDFs

Table 8.15 Change in LLDFs due to diaphragm location in Bridge B: (a) interior LLDFs and (b) exterior LLDFs

(a)

Diaphragm Location	Max Int. LLDF	AASHTO Int. LLDF	AASHTO Standard LLDF
None	0.314	0.33	0.705
Endspan	0.318	0.33	0.705
Midspan	0.319	0.33	0.705
Both	0.298	0.33	0.705

(b)

Diaphragm Location	Max Ext. LLDF	AASHTO Ext. LLDF	AASHTO Standard LLDF
None	0.327	0.438	0.705
Endspan	0.344	0.438	0.705
Midspan	0.349	0.438	0.705
Both	0.320	0.438	0.705

8.3.3 Deck Width

The deck width was varied by adding or removing DT girders to or from the existing bridge. The number of girders varies from five to nine. The effect of deck width on LLDFs for Bridge A can be seen in Figure 8.6a and 8.6b for interior and exterior girders. Detailed change in LLDFs for this bridge can be seen in Table 8.7. From the analytical LLDF values, there is no clear indication of the effect that the deck width has on DT girder bridges with damage. An interesting result shows that the interior LLDF increases by 12% when nine girders are used. The girder with this LLDF is the girder that exceeded the AASHTO LRFD for Bridge A, implying that the longitudinal joint damage is the reason for this high LLDF.

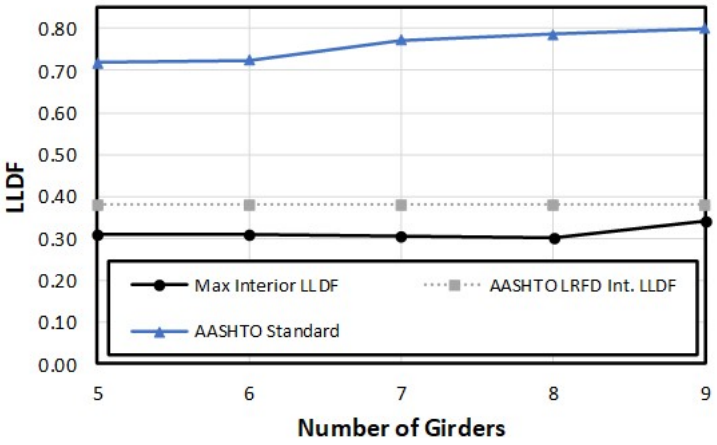

(a)

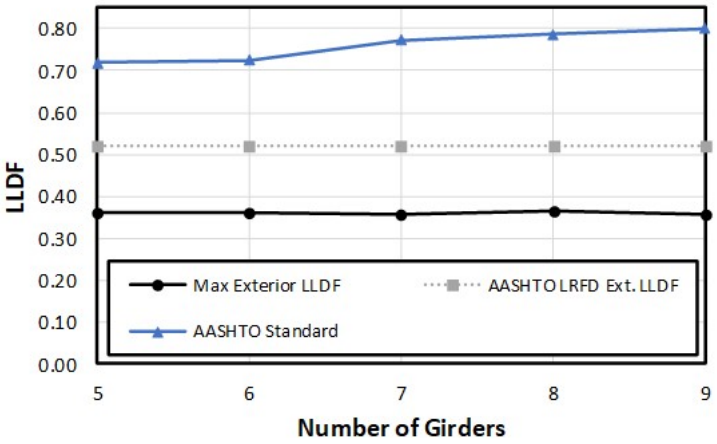

(b)

Figure 8.25 Change in LLDFs due to deck width in Bridge A: (a) interior LLDFs and (b) exterior LLDFs

Table 8.16 Change in LLDFs due to deck width in Bridge A: (a) interior LLDFs and (b) exterior LLDFs

(a)

Number of Girders	Max Int. LLDF	AASHTO LRFD Int. LLDF	AASHTO Standard LLDF
9	0.342	0.38	0.8
8	0.303	0.38	0.787
7	0.303	0.38	0.773
6	0.308	0.38	0.725
5	0.309	0.38	0.718

(b)

Number of Girders	Max Ext. LLDF	AASHTO LRFD Ext. LLDF	AASHTO Standard LLDF
9	0.358	0.52	0.8
8	0.364	0.52	0.787
7	0.358	0.52	0.773
6	0.362	0.52	0.725
5	0.362	0.52	0.718

The effect of deck width on the LLDFs for Bridge B can be seen in Figure 8.7 and Table 8.8. The AASHTO LRFD LLDFs are consistent with the analytical LLDFs for both interior and exterior girders, but still conservative. The same results occurred as they did in Bridge A. When the bridge has nine girders the interior LLDF increased by less than two-hundredths. According to the figures and tables, there is no significant correlation between the deck width on the studied bridges and the LLDFs. This is logical for a DT with significant longitudinal joint damage. If the load distribution is poor, then adding more girders would not change LLDFs significantly. Again, the AASHTO Standard LLDFs due to the change in the deck width are substantially larger than those from the analytical models.

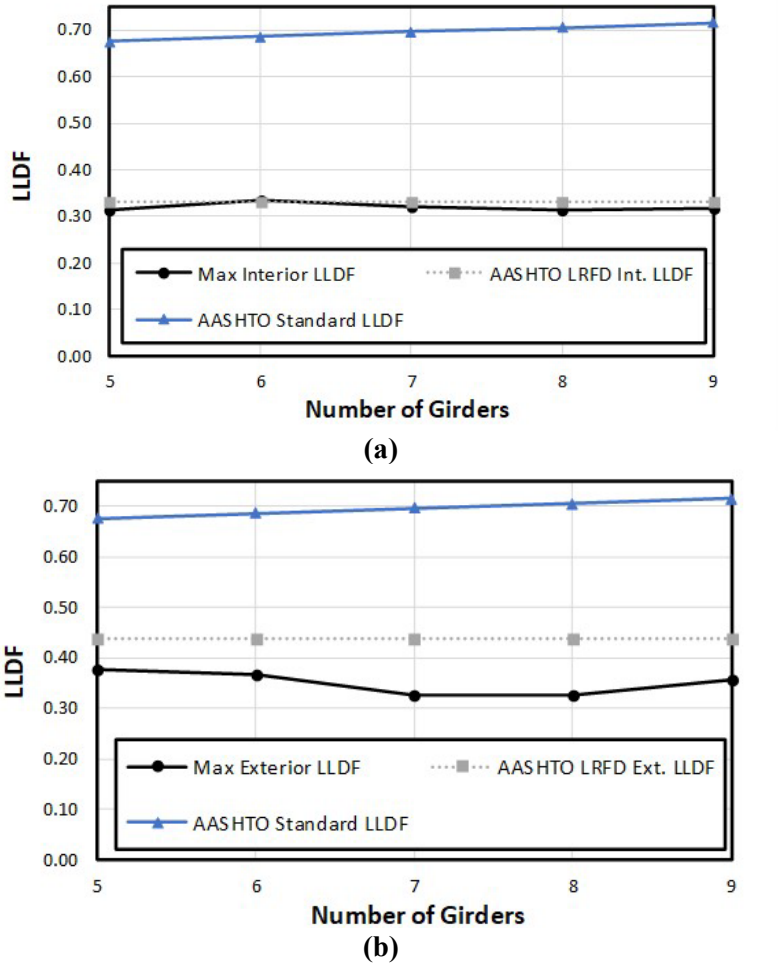

Figure 8.26 Change in LLDFs due to deck width in Bridge B: (a) interior LLDFs and (b) exterior LLDFs

Table 8.17 Change in LLDFs due to deck width in Bridge B: (a) interior LLDFs and (b) exterior LLDFs

(a)

Deck Width	Max Int. LLDF	AASHTO LRFD Int. LLDF	AASHTO Standard LLDF
9	0.318	0.330	0.715
8	0.314	0.330	0.705
7	0.320	0.330	0.696
6	0.336	0.330	0.686
5	0.312	0.330	0.676

(b)

Deck Width	Max Ext. LLDF	AASHTO LRFD Ext. LLDF	AASHTO Standard LLDF
9	0.357	0.438	0.715
8	0.327	0.438	0.705
7	0.324	0.438	0.696
6	0.368	0.438	0.686
5	0.375	0.438	0.676

8.3.4 Concrete Strength

The concrete strength of the DT girders was investigated to see if it impacted the LLDFs. The interior and exterior LLDFs for Bridge A can be seen in Figure 8.8a and 8.8b and the corresponding values in Table 8.9a and 8.9b. The only change that occurred was when the concrete compressive strength was 41.37 MPa. Both the interior and the exterior LLDFs increased. However, it only increased by 2.3% and 3.3%, respectively. This may imply that high strength concrete may have higher LLDFs, but for typical compressive strength values, it has very little effect.

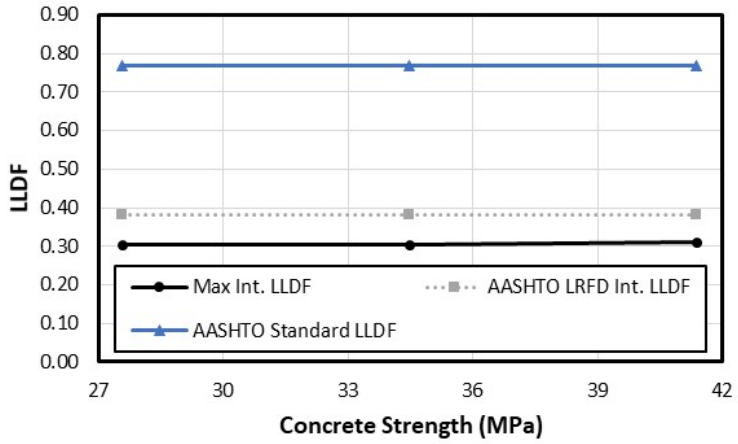

(a)

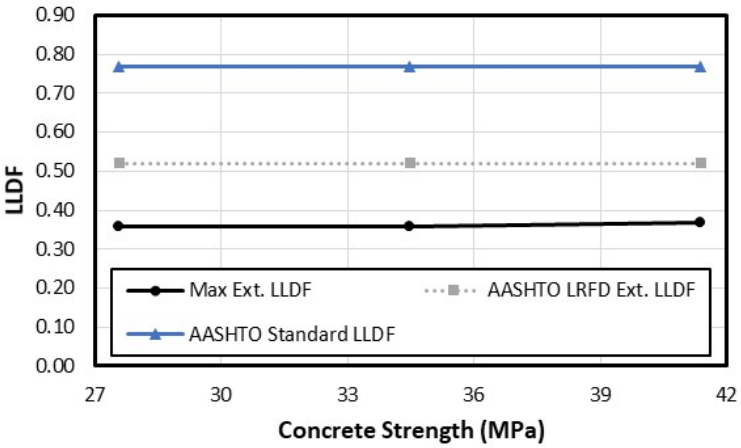

(b)

Figure 8.27 Change in LLDFs due to concrete strength in Bridge A: (a) interior LLDFs and (b) exterior LLDFs

Table 8.18 Change in LLDFs due to concrete strength in Bridge A: (a) interior LLDFs and (b) exterior LLDFs

(a)

f'c (MPa)	Max Int. LLDF	AASHTO LRFD INT. LLDF	AASHTO Standard LLDF
27.58	0.303	0.38	0.768
34.47	0.303	0.38	0.768
41.37	0.310	0.38	0.768

(b)

f'c (MPa)	Max Ext. LLDF	AASHTO LRFD Ext. LLDF	AASHTO Standard LLDF
27.58	0.358	0.52	0.768
34.47	0.358	0.52	0.768
41.37	0.370	0.52	0.768

For Bridge B, the interior and exterior LLDFs of the analytical model and two AASHTO specifications are shown in Figure 8.9a and 8.9b and Table 8.10a and 8.10b. There are very minimal changes between f'_C = 41.37 MPa and f'_C = 37.92 MPa (<2%). However, when f'_C = 27.58, both the interior and exterior LLDFs increased by 2.8% and 3.6%, respectively. Overall, the concrete strength has no significant effect on the LLDFs of DT girder bridges. It appears that the analytical LLDFs due to the increase in the concrete strength are much lower than those gained from the AASHTO Standard specifications.

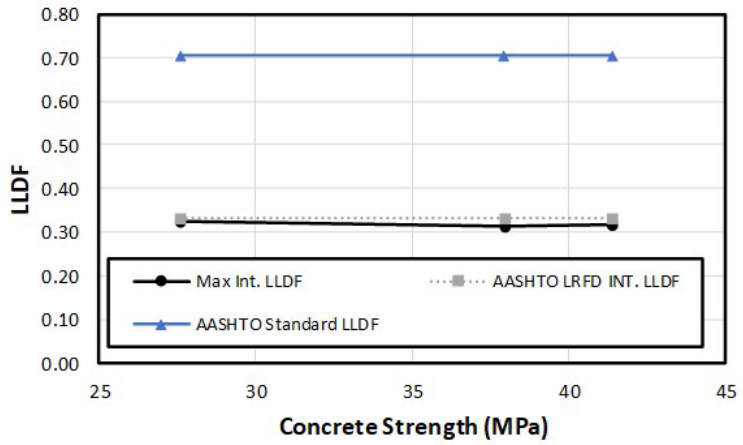

(a)

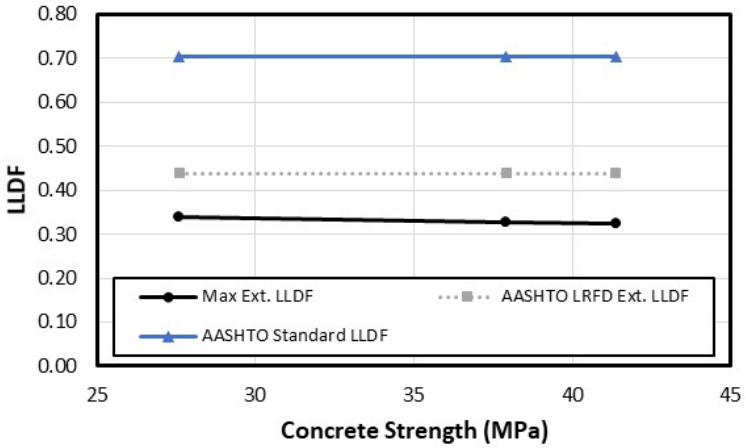

(b)

Figure 8.28 Change in LLDFs due to concrete strength in Bridge B: (a) interior LLDFs and (b) exterior LLDFs

Table 8.19 Change in LLDFs due to concrete strength in Bridge B: (a) interior LLDFs and (b) exterior LLDFs

(a)

f'c (MPa)	Max Int. LLDF	AASHTO LRFD INT. LLDF	AASHTO Standard LLDF
27.58	0.323	0.33	0.705
37.92	0.314	0.33	0.705
41.37	0.318	0.33	0.705

(b)

f'c (MPa)	Max Ext. LLDF	AASHTO LRFD Ext. LLDF	AASHTO Standard LLDF
27.58	0.339	0.438	0.705
37.92	0.327	0.438	0.705
41.37	0.324	0.438	0.705

8.3.5 Width-Length Ratio

The effect of the width to length ratio on the LLDFs was investigated in this study. For Bridge A, change in the interior and exterior LLDFs can be seen in Figure 8.10a and 8.10b. Table 8.11a and 8.11b summarize all detailed LLDFs for the interior and exterior girders. As the width to length ratio increases, so do the LLDFs. The AASHTO LRFD interior LLDFs show a similar pattern to the analytical interior LLDFs but are slightly conservative compared with the AASHTO values. The maximum percent difference is 25.7%. The AASHTO exterior LLDFs are significantly higher than the analytical exterior LLDFs. The maximum percent difference between exterior LLDFs and the AASHTO LRFD exterior LLDF is 72%, which is too conservative.

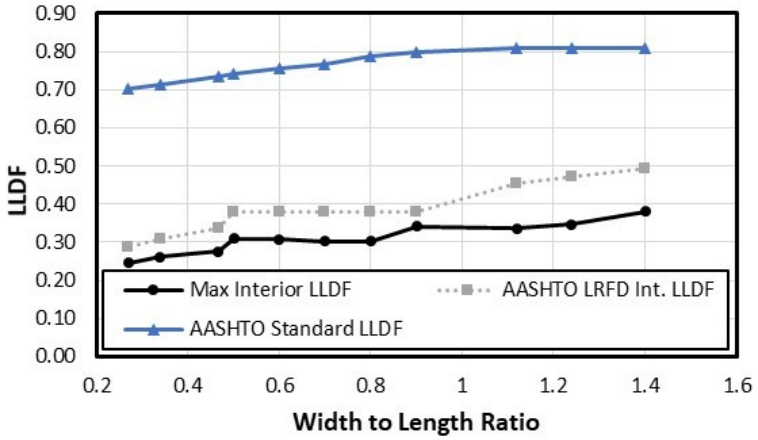

(a)

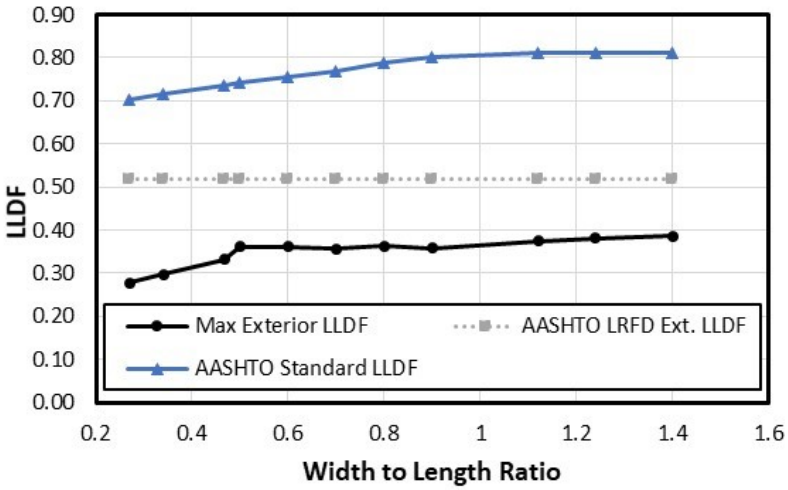

(b)

Figure 8.29 Change in LLDFs due to width-length ratio in Bridge A: (a) interior LLDFs and (b) exterior LLDFs

Table 8.20 Change in LLDFs due to width-length ratio in Bridge A: (a) interior LLDFs and (b) exterior LLDFs

(a)

W/L	Max Int. LLDF	AASHTO LRFD Int. LLDF	AASHTO Standard LLDF
1.40	0.380	0.492	0.811
1.24	0.347	0.472	0.811
1.12	0.336	0.455	0.811
0.90	0.342	0.38	0.800
0.80	0.303	0.38	0.787
0.70	0.303	0.38	0.768
0.60	0.308	0.38	0.757
0.50	0.309	0.38	0.741
0.47	0.275	0.338	0.736
0.34	0.262	0.308	0.715
0.27	0.245	0.287	0.703

(b)

W/L	Max Ext. LLDF	AASHTO LRFD Ext. LLDF	AASHTO Standard LLDF
1.40	0.386	0.520	0.811
1.24	0.381	0.520	0.811
1.12	0.374	0.520	0.811
0.90	0.358	0.520	0.800
0.80	0.364	0.520	0.787
0.70	0.358	0.520	0.768
0.60	0.362	0.520	0.757
0.50	0.362	0.520	0.741
0.47	0.333	0.520	0.736
0.34	0.297	0.520	0.715
0.27	0.278	0.520	0.703

The effect of width to length ratio on the interior and exterior LLDFs for Bridge B can be found in Figure 8.11a and 8.11b and Table 8.12a and 8.12b. Again, both interior and exterior LLDFs increase as the width-length ratio increases. However, the AASHTO LRFD LLDFs are more consistent with Bridge B until the width-length ratio is larger than 0.766. The interior LLDFs then exceed the AASHTO LRFD LLDFs because of the shear crack at girder G4, and G5 is the only girder to exceed the AASHTO LRFD LLDF values. The exterior AASHTO LRFD LLDFs are more conservative than the interior LLDFs. For the width-length ratio of 1.53, the analytical LLDFs slightly exceed the AASHTO LRFD exterior LLDFs. The AASHTO Standard LLDFs are significantly larger than the analytical LLDFs for both interior and exterior girders for Bridges A and B.

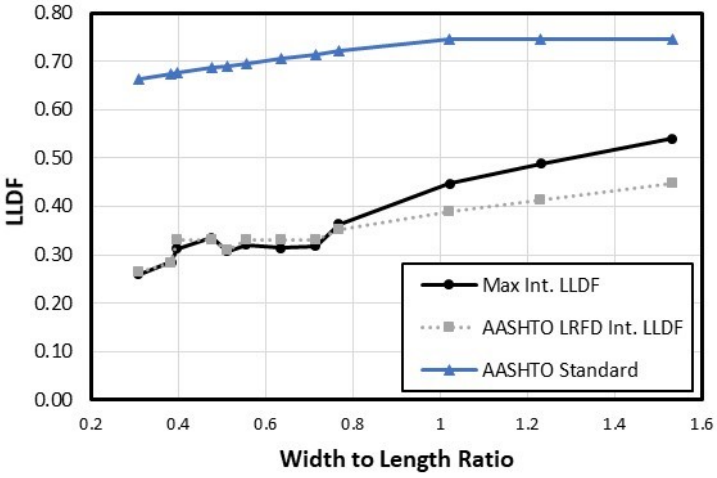

(a)

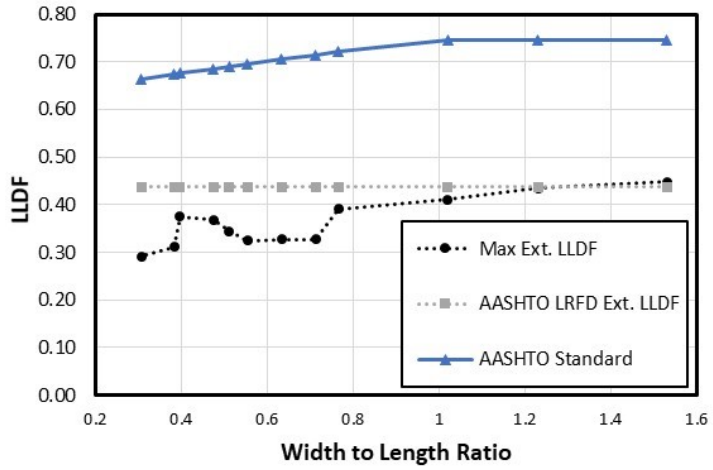

(b)

Figure 8.30 Change in LLDFs due to width-length ratio in Bridge B: (a) interior LLDFs and (b) exterior LLDFs

Table 8.21 Change in LLDFs due to width-length ratio in Bridge B: (a) interior LLDFs and (b) exterior LLDFs

(a)

W/L	Max Int. LLDF	AASHTO LRFD Int. LLDF	AASHTO Standard
1.53	0.540	0.447	0.747
1.23	0.488	0.414	0.747
1.02	0.447	0.389	0.747
0.766	0.363	0.353	0.721
0.713	0.318	0.330	0.715
0.634	0.314	0.330	0.705
0.554	0.320	0.330	0.696
0.511	0.307	0.309	0.69
0.475	0.336	0.330	0.686
0.396	0.312	0.330	0.676
0.383	0.285	0.282	0.674
0.307	0.259	0.263	0.664

(b)

W/L	Max Ext. LLDF	AASHTO LRFD Ext. LLDF	AASHTO Standard
1.53	0.448	0.438	0.747
1.23	0.435	0.438	0.747
1.02	0.411	0.438	0.747
0.766	0.391	0.438	0.721
0.713	0.328	0.438	0.715
0.634	0.327	0.438	0.705
0.554	0.324	0.438	0.696
0.511	0.345	0.438	0.69
0.475	0.368	0.438	0.686
0.396	0.375	0.438	0.676
0.383	0.312	0.438	0.674
0.307	0.292	0.438	0.664

It is important to notice that the analytical exterior LLDFs decrease with span length, even when it is not considered when calculating the AASHTO LRFD exterior LLDFs. Even though this analysis shows a trend, it appears that the width-length ratio affects the LLDF because of the change in span length. It was previously found that width has little effect. However, the width to length ratio may be a good indication that bridge rating engineers should investigate the damage and LLDFs more in depth.

9. SUMMARY, CONCLUSIONS, AND FUTURE WORK

This study discussed the structural performance of deteriorating double-tee (DT) girder bridges that have been in service for many years. This included field testing of two single-span DT girder bridges in South Dakota for live load distribution factors (LLDFs) and dynamic load allowance (IM) factors. These bridges encompassed Bridges A with seven 762-mm-deep prestressed DT girders and Bridge B having eight 584-mm-deep girders. An investigation into the determination of LLDFs for individual DT girders for Bridges A and B was conducted using three approaches: girder, stem, and joint. The damage on Bridges A and B was then inspected and quantified for use in the analytical analysis of their finite element models. Each model was calibrated with field data. With the calibrated models, a parametric study was conducted on the LLDFs of Bridges A and B with different design parameters. The considered parameters were span length, location of diaphragms, concrete strength, deck width, and width-length ratio. The following conclusions were determined for both bridges based on the findings presented in this study.

1. LLDFs calculated using the AASHTO LRFD approach were generally conservative compared with the field LLDFs. There were only two instances, one on each bridge, that the field LLDFs slightly exceeded those from the AASHTO LRFD. Bridge A exceeded the LRFD value on G7 (an exterior girder) by 2.6% and Bridge B exceeded the LRFD value on G5 (an interior girder) by 2.9%.
2. LLDFs calculated using the AASHTO Standard significantly exceeded those from the field testing and also AASHTO LRFD for both bridges. The AASHTO Standard specifications had an average percent difference from the field LLDFs of approximately 90% for both deteriorating DT bridges.
3. Both the AASHTO LRFD and AASHTO Standard specifications overestimated the IM for the two DT bridges tested. The peak IM from the field tests was 50% lower than that from two AASHTO values. Therefore, the two specifications offered overly conservative approaches to estimate IM for DT bridges with significant deterioration.
4. The girder approach was the most accurate approach to calculating the AASHTO Specification-compliant LLDFs of both DT girder bridges. The percent differences, when compared with AASHTO LRFD and AASHTO Standard, were 34% and 91%, respectively. The joint approach was nearly as accurate as the girder approach. However, they may not always be conservative when compared to the AASHTO LRFD specifications.
5. The stem approach was the most conservative of the three approaches relative to the AASHTO LRFD and AASHTO Standard specifications, with average percent differences of 58% and 87%, respectively. This approach also showed a similar pattern between the AASHTO LRFD LLDFs and the field LLDFs. The interior stem of the exterior girder yielded higher LLDFs than the exterior stem of the exterior girder due to the position of the loading.
6. The AASHTO Standard specifications were significantly higher than the field values. The average percent differences were above 80% for every approach considered in this study. However, there was one outlier. One AASHTO Standard LLDF value compared with the stem approach was not conservative. It was proven that there was significant joint damage near this stem, explaining the large field LLDFs.
7. From the parametric study, it was found that the AASHTO LRFD interior LLDFs were typically consistent with the analytical interior LLDFs, if not conservative for DT girder bridges with significant longitudinal joint damage. However, when Bridge B had small spans (i.e., less than 12.2 meters), the AASHTO LRFD interior LLDFs were not sufficiently conservative. The AASHTO LRFD exterior LLDFs were conservative for the DT girder bridges with significant

longitudinal joint damage. The AASHTO Standard LLDFs were over-conservative for all cases investigated during this parametric study.

8. The concrete strength, deck width, and diaphragm location did cause some variation in LLDFs, but the values were not significant. When diaphragms were present at the endspan and midspan, there was some variation (5% on average). It is reasonable to conclude that these parameters did not have a significant effect on the LLDFs of a DT girder bridge with significant joint damage.
9. Both the interior and exterior LLDFs decrease as the span length increases. The interior LLDF decreased by 10.8% per 6.1 m of span, on average, for Bridge A. The exterior LLDF decreased by 8.1% per 6.1 m of span, on average. The interior LLDF decreased by 8.5% per 6.1 m of span, on average, for Bridge B. The exterior LLDF decreased by 5.8% per 6.1 meters of span, on average, for Bridge B. This agrees with the AASHTO LRFD interior LLDF equation. However, the AASHTO LRFD exterior LLDFs do not decrease with span length since the lever rule is used. This may be an over-conservative approach.
10. The width-length ratio demonstrated an impact on the LLDFs. However, considering the deck width did not affect the LLDFs, it is reasonable to believe that this impact was due to the change in span length and not specifically the width-length ratio. At the width-length ratio larger than 0.766 on Bridge B, the interior LLDFs exceeded the AASHTO LRFD LLDFs due to a shear crack in one of the girders. The width-length ratio may be an important indicator to bridge rating engineers to evaluate the load-carrying capacity using LLDFs for deteriorating DT bridges.

The study shown above provided a basis for more investigations into the structural performance of DT bridges. More studies should be conducted to study the effects of the different geometries of the DT girder since many different configurations of DT girders are available. Also, further studies can be conducted to investigate LLDFs specific to joints and stems to create a more accurate method for calculating LLDFs for DT girder bridges. Calculating LLDFs via stems, similar to the stem approach, matched the strain pattern of the field LLDFs. This is promising; however, the method for determining design LLDFs would need to be investigated to improve the accuracy of the AASHTO LLDF design equations. Finally, a further parametric study for the IM factors is needed by modifying the analytical models presented for the LLDF calculation taking into account the truck suspension system.

REFERENCES

AASHTO LRFD. (2012). "AASHTO LRFD Bridge Design Specifications, Sixth Edition." American Association of State Highway and Transportation Officials (AASHTO), Washington, DC.

AASHTO. (2013). "Manual for Bridge Element Inspection." American Association of State Highway and Transportation Officials (AASHTO), Washington, D.C.

AASHTO. (1996). "Standard Specifications for Highway Bridges, Sixteenth Edition." American Association of State Highway and Transportation Officials (AASHTO), Washington, D.C.

Ashebo, D. B., Chan, T. H., and Yu, L. (2007). "Evaluation of dynamic loads on a skew box girder continuous bridge Part II: Parametric study and dynamic load factor." *Engineering Structures*, 29(6), 1064–1073.

Deng, L., Yang, Y., Zou, Q., and Cai, C.S. (2014). "State-of-the-art review of dynamic impact factors of highway bridges." *J. Bridge Engineering*, ASCE, 20(5).

Huang, J., and Davis, J. (2018). "Live load distribution factors for moment in next beam bridges." *Journal of Bridge Engineering*, 23(3), 06017010.

Hodson, D., Barr, P. and Halling. M., (2012). "Live-load analysis of posttensioned box-girder bridges." *J. Bridge Eng.* 17 (4): 644–651. https://doi .org/10.1061/(ASCE)BE.1943-5592.0000302.

Kidd, B. (2019). "Field and Numerical Study for Deteriorating Precast Double-Tee Girder Bridges." M.S. Thesis, South Dakota State University.

Kidd, B., Rimal, S., Seo, J., Tazarv, M., and Wehbe, N., (2021). "Field Testing of Deteriorating Double Tee Girder Bridges for Determination of Live Load Distribution Factors and Dynamic Load Allowance." *Structural Engineering and Mechanics, In Review.*

Kim, S., and Nowak, A. S., (1997). "Load distribution and impact factors for I-girder bridges." *Journal of Bridge Engineering.* https://doi.org/10.1061/(ASCE)1084-0702(1997)2:3(97)

PCI. (2003). "PCI Bridge Design Manual," Precast/Prestressed Concrete Institute, Chicago, IL.

PCINE. (2012). "Guidelines for northeast extreme tee beam (NEXT Beam), First Edition," Precast Concrete Institute Northeast (PCINE), Belmont, MA.

Rimal, S., Kidd, B., Tazarv, M., Seo, J., and Wehbe, N., (2019). *Methodology for Load Rating Double-Tee Bridges*, MPC-19-398. North Dakota State University - Upper Great Plains Transportation Institute, Fargo: Mountain-Plains Consortium.

Rimal, S., Kidd, B., Tazarv, M., Seo, J., and Wehbe, N., (2020). "Methodology for Load Rating of Damaged Double-Tee Girder Bridges." *Journal of Bridge Engineering*, 26(1), 04020110.

Seo, J., and Hu, J. W. (2014). "Simulation-based load distribution behavior of a steel girder bridge under the effect of unique vehicle configurations." *European Journal of Environmental and Civil Engineering,* 18(4), 457-469.

Seo, J., and Hu, J. W. (2015). "Influence of atypical vehicle types on girder distribution factors of secondary road steel-concrete composite bridges." *Journal of Performance of Constructed Facilities*, 29(2), 04014064.

Seo, J., Kilaru, C. T., Phares, B., and Lu, P. (2017). "Agricultural vehicle load distribution for timber bridges." *Journal of Bridge Engineering*, 22(11), 04017085.

Seo, J., Phares, B., and Wipf, T. J. (2014a). “Lateral live-load distribution characteristics of simply supported steel girder bridges loaded with implements of husbandry.” *Journal of Bridge Engineering*, 19(4), 04013021.

Seo, J., Phares, B., Dahlberg, J., Wipf, T. J., and Abu-Hawash, A. (2014b). “A framework for statistical distribution factor threshold determination of steel–concrete composite bridges under farm traffic.” *Engineering Structures*, 69, 72-82.

Shinozuka, M., Feng, M. Q., Lee, J., and Naganuma, T. (2000). “Statistical analysis of fragility curves.” *Journal of Engineering Mechanics*, 126(12), 1224–1231.

Singh, A. K. (2012). "Evaluation of live-load distribution factors (LLDFs) of next beam bridges" Master’s Theses - February 2014. 816.

Tazarv, M., Bohn, L., Wehbe, N. (2019). “Rehabilitation of longitudinal joints in double-tee bridges,” *Journal of Bridge Engineering*, ASCE, DOI: 10.1061/(ASCE)BE.1943-5592.0001412, 15 pp.

Torres, V.J. (2016) /(ASCE)BE.1943-5592.0001412, 15 pp. of longitudinal joints in double-tee br.” MS Thesis, Utah State University, Civil and Environmental Engineering Department, Logan, Utah.

Wehbe, N., Konrad, M., and Breyfogle, A. (2016). “Joint Detailing Between Double Tee Bridge Girders for Improved Serviceability and Strength.” *Transportation Research Record: Journal of the Transportation Research Board*, No. 2592, Transportation Research Record, Washington, D.C, 2592(1), 108-116.

Yousif, Z., and Hindi, R. (2007). “AASHTO-LRFD Live Load Distribution for Beam-and-Slab Bridges: Limitations and Applicability.” *Journal of Bridge Engineering*, 12(6), 765–773.

Zokaie, T. (2000). “AASHTO-LRFD live load distribution specifications.” *Journal of Bridge Engineering*, 5(2), 131–138.